

Filamin A in Cardiovascular Remodeling

Sashidhar Bandaru

Department of Medical Biochemistry and Cell Biology
Institute of Biomedicine
Sahlgrenska Academy, University of Gothenburg



UNIVERSITY OF GOTHENBURG

Gothenburg, 2018

Cover illustration by Sashidhar Bandaru

Filamin A in Cardiovascular Remodeling

© Sashidhar Bandaru, 2018
sashidar.bandaru@medkem.gu.se

ISBN 978-91-7833-229-8 (Print)
ISBN 978-91-7833-230-4 (PDF)

Printed in Gothenburg, Sweden, 2018
Printed by BrandFactory

To my dear parents, Sekhar, Lakshmi, my wife Srujana and my son Shriyan

Filamin A in Cardiovascular Remodeling

Sashidhar Bandaru

Department of Medical Biochemistry and Cell Biology

Institute of Biomedicine

Sahlgrenska Academy, University of Gothenburg

Göteborg, Sweden

ABSTRACT

Filamin A (FLNA) is a large actin-binding cytoskeletal protein that stabilizes actin networks and integrates them with cell membranes. FLNA is therefore important for cell motility and organ development. We recently discovered that a C-terminal fragment of FLNA (FLNA^{CT}) can be cleaved off by calpain and stimulate angiogenesis by transporting transcription factors into the nucleus. However, little is known about the role of FLNA in cell types that participate in the pathogenesis of vascular diseases where angiogenesis typically plays an important role. In this thesis, we defined the impact of inactivating *Flna* in mouse vascular endothelial cells and macrophages on the pathogenesis of myocardial infarction (MI) and atherosclerosis, respectively—and made several exciting discoveries.

In Study I, we induced MI by ligating the left descending coronary artery in *wt* control mice and mice lacking FLNA in endothelial cells. The *Flna*-knockout mice developed larger MI lesions than controls, and exhibited larger and thinner left ventricles, impaired cardiac function, elevated plasma levels of the cardiac damage biomarker NT-proBNP, and reduced plasma levels of the angiogenesis-promoting factor VEGF-A. Hearts from the *Flna*-knockout mice exhibited reduced capillary structures within infarcted regions; and cultured *Flna*-deficient endothelial cells showed impaired migration and tubular formation, along with reduced levels of the signaling molecules p-ERK and p-AKT and the small GTPase RAC1.

In Study II, we first discovered that FLNA expression was higher in human carotid arteries with advanced atherosclerotic plaques than with intermediate plaques. We generated mice lacking FLNA in macrophages and found that their macrophages proliferated and migrated less compared with littermate controls. Moreover, *Flna*-deficient macrophages exhibited reduced levels of p-ERK and p-AKT, and reduced lipid uptake and increased cholesterol efflux. In two different mouse atherosclerosis models, the knockout of FLNA in macrophages markedly reduced lesion size and number of CD68-positive lesional macrophages. Interestingly, the calpain-cleaved FLNA^{CT} fragment interacted strongly with STAT3 in *wt* macrophages. Inhibiting FLNA cleavage with the calpain inhibitor calpeptin reduced nuclear p-STAT3 levels and subsequent IL-6 secretion *in vitro*; and reduced atherosclerotic lesions *in vivo*.

We conclude that FLNA interacts with transcription factors and thereby regulates angiogenesis and inflammatory responses which are important events in the progression of MI and atherosclerosis. These findings identify FLNA as an important new mediator of cardiovascular remodeling and as a potential target for therapy.

Keywords: cytoskeleton, myocardial infarction, atherosclerosis

ISBN 978-91-7833-229-8 (Print)

ISBN 978-91-7833-230-4 (PDF)

Betydelsen av Filamin A

för Remodellering vid Hjärt-kärlsjukdomar

Sashidhar Bandaru

Avdelningen för medicinsk kemi och cellbiologi
Institutionen för biomedicin
Sahlgrenska akademien, Göteborgs universitet
Göteborg, Sweden

SAMMANFATTNING

Vid hjärt-kärlsjukdomar kan skador påverka kroppens kärlceller vilket under läkeprocessen leder till nybildning av blodkärl — en process som kallas angiogenes. Att styra angiogenes med läkemedel eller andra strategier skulle ge möjlighet att i högre grad reparera de skador som uppkommer vid t.ex. hjärtinfarkt och åderförfattning. Angiogenes styrs av proteiner som påverkar uttrycket av cellernas gener. Vår grupp har upptäckt att ett protein som kallas filamin A (FLNA), interagerar med flera av dessa faktorer och om FLNA inte fungerar under fosterutvecklingen leder det till hög dödlighet på grund av försämrade angiogenes.

Målsättningen med studierna i denna avhandling var att ta reda på om FLNA i blodkärlceller kan stimulera nybildning av blodkärl efter hjärtinfarkt och att avgöra om hämning av FLNA i den inflammatoriska celltypen makrofager kan minska utvecklingen av åderförfattning.

Uttrycket av FLNA har studerats i humana vävnader som har varit utsatta för hjärtinfarkt och halspulsåderateroskleros. Möss som saknar FLNA i kärlets endotelceller har studerats för angiogenes efter hjärtinfarkt eller makrofager för cellfunktion vid utvecklandet av åderförfattning. I odlade celler från dessa möss och i humana celler, i vilka uttrycket av FLNA är blockerat, har vi jämfört cellens förmåga att föröka sig, vandra, bilda nya blodkärl, utsöndra cytokiner och ta upp fett. Blockering av FLNA i endotelceller ledde till minskad celltillväxt och migrering, och minskad nybildning av kärl i odlade celler, vilket ledde till större infarktvolym och förvärrad hjärtsvikt hos möss. Avsaknad av FLNA i makrofager ledde till försämrade cellmigrering, utsöndring av anti-inflammatoriska cytokiner samt fettupptagning i odlade makrofager och således ledde till mindre aterosklerotiska fettplack hos möss. Vi har identifierat signalmolekyler eller transkriptionsfaktorer som regleras av FLNA-proteinet, vilket ger möjlighet till utveckling av nya, riktade behandlingar. Vi har även upptäckt att spjälkning av FLNA med enzymet calpain har betydelse för makrofagfunktionen. Vid kemisk hämning av detta enzym utvecklade möss mindre aterosklerotiska fettplack.

Betydelsen av FLNA för hjärtinfarkt och åderförfattning har hittills varit okänd. Kunskapen som har genererats i denna avhandling kan få stor betydelse för behandling av allvarliga hjärt-kärlsjukdomar inom sjukvården. En direkt tillämpning av vår forskning kan vara utveckling av nya prognostiska markörer för hjärt-kärlsjukdomar. Dessutom skulle en artificiellt kontrollerad angiogenes ge en möjlighet att i större grad reparera de skador som uppkommer vid t.ex. hjärtinfarkt, stroke eller accelererad åderförfattning.

List of publications

This thesis is based on the following publications below:

Study I

Deficiency of filamin A in endothelial cells impairs left ventricular remodeling after myocardial infarction in mice.

Bandaru S, Grönros J, Redfors B, Zhou A-X, Larsson E, Çil Ç, Ömerovic E, Akyürek LM.
Cardiovascular Research 2014, 105:151-9

Study II

Deficiency of filamin A impairs macrophage function and reduces atherosclerotic plaque size.

Bandaru S, Salimi R, Ala C, Akula MK, Ekstrand M, Devarakonda S, Karlsson J, Levin M, Borén J, Bergo MO, Akyürek LM.
Under revision 2018

Additional publications not included in this thesis

1. Targeting the protein filamin A efficiently reduces *Kras2*-induced lung adenocarcinomas and endothelial response to tumor growth. Nallapalli RK, Ibrahim M, **Bandaru S**, Zhou A-X, Pazooki D, Borén J, Bergo MO, Akyürek LM.
Molecular Cancer 2012, 11:50.
2. Targeting filamin B induces tumor growth and metastasis via enhanced activity of matrix metalloproteinase-9 and secretion of VEGF-A. **Bandaru S**, Zhou A-X, Rouhi P, Zhang Y, Bergo MO, Cao Y, Akyürek LM.
Oncogenesis 2014, 3:e119.
3. Transcriptomic profiling of primary neuroblastomas reveals a high-risk tumor associated long noncoding RNA NBAT1, with functional roles in cell proliferation and neuronal differentiation. Pandey GK, Mitra S, Subhash S, Mishra K, Fransson S, Ganeshram A, Mondal T, **Bandaru S**, Akyürek LM, Kanduri M, Abrahamsson J, Pfeifer S, Larsson E, Martinsson T, Kogner P, Hedborg F and Kanduri C.
Cancer Cell 2014, 26:722–37.
4. p110 α hot spot mutations E545K and H1047R exert metabolic reprogramming independently of p110 α kinase activity. Chaudhari A, Krumlinde D, Lundqvist A, Akyürek LM, **Bandaru S**, Skälén K, Ståhlman M, Borén J, Wettergren Y, Ejeskär K, Rotter Sopasakis V.
Molecular and Cell Biology 2015, 35:3258–73.
5. Sense-Antisense lncRNA pair encoded by locus 6p22.3 determines neuroblastoma susceptibility via the USP36-CHD7-SOX9 regulatory axis. Mondal T, Juvvuna PK, Kirkeby A, Mitra S, Kosalai ST, Traxler L, Hertwig F, Wernig-Zorc S, Miranda C, Deland L, Volland R, Bartenhagen C, Bartsch D, **Bandaru S**, Engesser A, Subhash S, Martinsson T, Carén H, Akyürek LM, Kurian L, Kanduri M, Huarte M, Kogner P, Fischer M, and Kanduri C.
Cancer Cell 2018, 33:417–434.e7.
6. Blocking the cleavage of filamin A by calpain inhibitor decreases tumor cell growth. Salimi R, **Bandaru S**, Devarakonda S, Gökalp S, Ala C, Alvandian A, Yener N, Akyürek LM.
Anticancer Research 2018, 38:2079–2085.

Contents

Abbreviations	13
Filamin A	15
<i>Filamin A in cellular signaling</i>	16
<i>Filamin A in cellular migration</i>	18
<i>Interaction partners of filamin A</i>	19
<i>Integrins</i>	19
<i>GTPases</i>	20
<i>Transcriptional factors</i>	20
Calpains and calpain inhibitors	23
<i>Therapeutic uses of calpain inhibitors</i>	23
Mouse models of filamin A deficiency	24
Myocardial infarction	25
<i>Endothelial cells in myocardial infarction</i>	25
Atherosclerosis	26
<i>Macrophages in atherosclerosis</i>	26
Human mutations in filamin A gene	27
Aims	29
Methods	31
<i>Histology and image analysis</i>	31
<i>Conditional gene knockout strategy</i>	31
<i>Cell culture</i>	33
<i>Cells assays</i>	33
<i>Mouse model of myocardial infarction</i>	35
<i>Mouse model of atherosclerosis</i>	36
<i>Statistics</i>	36
Summary of results	36

<i>Study I: Deficiency of filamin A in endothelial cells impairs left ventricular remodeling after myocardial infarction.</i>	37
<i>Study II: Targeting filamin A reduces macrophage function and atherosclerotic plaques in mice.</i>	39
Discussion	43
Future directions	47
<i>Filamin A as a prognostic marker</i>	47
<i>Calpain inhibitors to treat atherosclerosis</i>	47
<i>Future experiments</i>	47
Acknowledgements	49
References	51

Abbreviations

ABD	Actin-binding domain
ABP	Actin-binding proteins
AR	Androgen receptor
ARFGEF2	ADP-ribosylation factor guanine exchange factor 2
CH	Calponin homology domain
CMG	Cardiomyocyte growth medium
CVD	Cardiovascular diseases
FLNA	Filamin A protein
FLNA ^{CT}	C-terminal fragment of filamin A
FLNA ^{NT}	N-terminal fragment of filamin A
FLNB	Filamin B protein
FLNC	Filamin C Protein
<i>FLNA</i>	Human filamin gene
<i>Flna</i>	Mouse filamin A gene
FILIP	Filamin A interacting protein 1
F-actin	Filamentous actin
GP	Glycoprotein
GEF	Guanine nucleotide-exchange factor
GTP	Guanosine triphosphate
HIF-1 α	Hypoxia-inducible factor-1 α
H	Hinge domain of FLNA
HUVEC	Human umbilical vein endothelial cells
IL-6	Interleukin-6
Ig	Immunoglobulin
LDL	Low-density lipoproteins
<i>Ldlr</i>	Mouse low-density lipoprotein receptor gene
LPS	Lipopolysaccharide
LV	Left ventricle
MI	Myocardial infarction
MS1	Transformed mouse pancreatic endothelial cells
NT-proBNP	N-Terminal prohormone of brain natriuretic peptide
PVNH	Periventricular nodular heterotopia
PCSK9	Proprotein convertase subtilisin/kexin type-9
STAT3	Signal transducer and activator of transcription 3
siRNA	Small interfering RNA
VEGF-A	Vascular endothelial cell growth factor-A
<i>wt</i>	Wild-type
XVMD	X-linked myxoid valvular dystrophies

Filamin A

The actin cytoskeleton is mainly involved in the formation and maintenance of cell shape and morphology in response to external stimuli from surrounding connective tissue. Filamins are one of the actin-binding proteins (ABP) that mediate dynamic remodeling during cell locomotion. Furthermore, filamins are involved in cell signaling and transcription. In 1975, the first isoform of filamin proteins was discovered and purified in macrophages of chicken gizzard [1]. In 2000, the first splice variant of the filamins lacking an actin-binding domain (ABD) was identified in *Drosophila melanogaster* [2]. The filamin family comprises three members; filamin A (FLNA), filamin B (FLNB) and filamin C (FLNC). They all exhibit 70% homology with their amino acids and 45% homology in hinge 1 (H1) and hinge 2 (H2) regions [3]. To date, the most commonly studied isoform of filamins is FLNA. Both mouse *Flna* and the human *FLNA* gene are located on the X chromosome. Human *FLNB* and *FLNC* genes are located on chromosomes 3 and 7 respectively, whereas mouse *Flnb* and *Flnc* genes are located on chromosomes 14 and 6 respectively [4]. Although *FLNA* and *FLNB* are very similar to one another, the nature of mutations and clinical phenotypes associated with mutations differs. All three filamin isoforms are expressed strongly during development stages. In adult tissues, FLNA and FLNB are ubiquitously expressed throughout the body, whereas the expression of FLNC is restricted to skeletal and cardiac muscles [4].

The long elongated Y-shaped (240–280 kDa) polypeptide chain of FLNA can exist in either homo- or heterodimers. Each chain of FLNA is composed of 24 immunoglobulin (Ig) repeats which are separated by two hinge (H1 and H2) regions, whereas H1 comprises between 15–16 Ig-repeats and H2 between 23–24 Ig-repeats (Figure 1) [5]. These hinge regions are calpain sensitive and separate 24 Ig-repeats into the rod 1 domain which comprises 1–15 Ig-repeats, rod 2 comprising 16–23 Ig-repeats and a dimerization domain [6, 7]. Ig 24 is the most C-terminal repeat of FLNA (FLNA^{CT}), which not only helps to mediate the dimerization but also confers the Y-shape on the dimeric structure [8]. FLNA^{CT} is comprised of two filamin monomers and these monomers help to anchor the F-actin to the cell membrane through transmembrane receptors [7]. The rod 1 domain is transfixed to F-actin, whereas the rod 2 domain does not interact with F-actin. This allows rod 2 to set itself free and interact with multiple proteins involved in signal transduction. Most of the protein interactions are conferred on the rod 2 domain due to its free-moving structure [9].

ABD is the key subunit of FLNA, binding to F-actin. FLNA dissociates from F-actin due to the competitive binding of Ca²⁺-calmodulin, which results in the deletion of ABD in the FLNA subunit and weakens its ability to instigate gelation activity in the actin solution [9]. The ABD of FLNA is composed of two calponin homology (CH) domains, known as CH1 and CH2, which are separated by a linker. This organization of CH domains determines the binding ability of

FLNA actin molecules towards F-actin [3]. The amino acids from 121–147 in FLNA, which corresponds to the CH1 domain, serve as a primary binding site for F-actin [10]. The amino acid sequence of actin, where FLNA binding is conferred, also overlaps with many other actin-binding proteins, which suggests that FLNA competes with other actin-binding proteins. Upon binding to one another, the ABD of FLNA with actin, structural reorganization occurs, which could impact the shape of F-actin [7].

Purified FLNA protein under the electron microscope has shown the rod 2 domain as a folded structure and rod 1 as an elongated chain [11]. The long range of Ig-repeats in the rod 1 domain of FLNA provides essential flexibility during mechanical stress and Ig-repeats 9–15 containing ABD provide high-affinity binding towards F-actin. Ig-repeats 1–8 in the rod 1 domain are flexible and help the 9–15 Ig-repeats to provide the correct alignment with actin monomers [7]. Even though both rod 1 and rod 2 of FLNA have similar numbers of Ig-repeats, the Ig-repeats of rod 2 form a compact shape far more than those in the rod 1 domain. The binding of even numbered repeats to the neighboring repeats in FLNA results in a compact, more globular structure of rod domains [12, 13]. The hinge regions in the human FLNA protein have a larger amino acid assortment and are also longer, which not only provides extra flexibility in sheer stress but also helps with binding to actin at a perpendicular angle, even though actin is widely spread [14]. The hinge regions are proteolyzed by Ca^{2+} -dependent calpains and the cleavage of these

sites produces a 90 kDa FLNA^{CT} and a 200 kDa N-terminal fragment (FLNA^{NT}) [15].

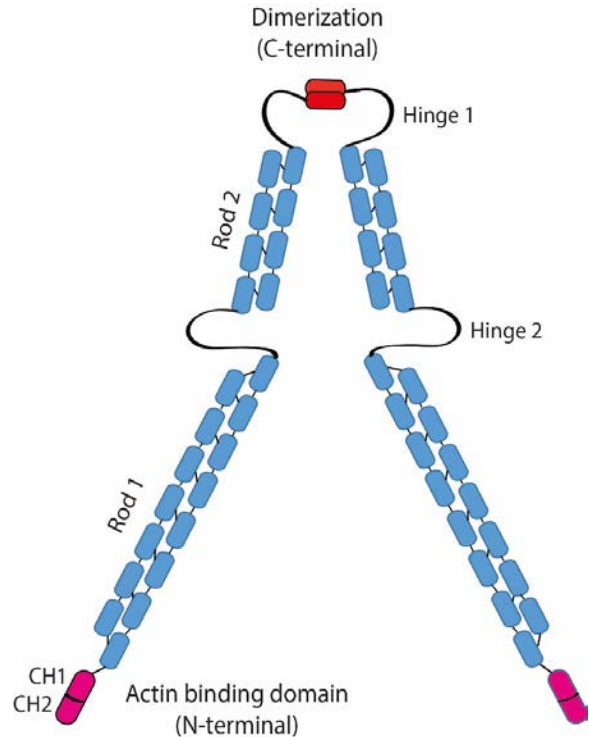


Figure 1: Structure of filamin A. FLNA homodimers include an N-terminal actin-binding domain, a C-terminal dimerization domain and 24 Ig-repeats that are interrupted by hinge 1 and hinge 2 regions.

Filamin A in cellular signaling

Filamin A is a large protein and mainly helps to provide scaffolding to its interacting partners. Due to the high level of similarity between the Ig-repeats, multiple proteins bind at multiple sites of FLNA [11]. Other than providing a structural organization to cells, FLNA protein is also involved in various other functions, such as organ development, cell signaling, migration, proliferation, cell adhesion, phosphorylation, transcription and the nuclear transportation of

transcriptional factors. Many studies reveal that various cellular functions are performed by FLNA through its interaction with more than 90 proteins [16]. FLNA is found to be co-localized with tissue factor (TF), which is also regarded as a ligand to the cytoplasmic domain of TF [17]. The absence of interacted FLNA–TF might be one of the causes of embryonic lethality in *Flna*-deficient mice, due to the incomplete implantation of the embryo into the endometrium and the covering of the location with a fibrin plug [18]. FLNA promotes platelet adhesion by interacting with glycoprotein-Ib α (GPIb α) [19]. Studies have shown that FLNA is also associated with the regulation of cell cycles. *Flna*-deficient mouse embryos exhibit a smaller brain size and fewer neuronal progenitors, which contribute to a prolonged cell cycle [20]. This prolonged cell cycle occurs mainly in the M phase, due to the interaction of FLNA with CDK1 kinase and WEE1. In the absence of FLNA, the phosphorylation of CDK1 kinase is increased, resulting in a prolonged cell cycle [20].

There are a few protein interactions which can alter the expression and functionality of the FLNA protein. The interaction of FLNA with FLNA-interacting protein (FILIP) promotes cortical radial cell migration from the ventricular zone [21]. When *FLNA* is overexpressed in cells silenced for *FILIP* by siRNA, it regulates cell polarity in intermediate and subventricular zones in the neo cortex [22]. FLNA binding with the ADP-ribosylation factor, guanine exchange factor 2 (ARFGEF2), transports FLNA to the cell surface in neuronal progenitors and the

silencing of *ARFGEF2* inhibits the transport of FLNA in the Golgi apparatus [23]. FLNA interacts with REFILINB and forms a complex. This complex organizes perinuclear actin bundles by forming an actin cap. The FLNA–REFILINB complex is also able to alter its nuclear shape during epithelial-mesenchymal transition [24]. FLNA interaction with MEKK4 is also important to promote neuronal migration. Like *FLNA* human mutation, *MEKK4*-deficient mice develop PVNH and FLNA expression levels that are more elevated in the forebrain in these mice [25]. Interaction with cyclin D1 of FLNA promotes breast cancer cell migration and invasiveness [26]. FLNA binding to the androgen receptor (AR) helps the nuclear localization of AR and inactivates AR protein when it enters the nucleus [27]. This FLNA–AR interaction may also promote cancer progression in prostate cancer [28]. FLNA interaction with BRCA2 helps to provide scaffolding to BRCA2 during the assembly of DNA repair [29]. Phosphorylated ERK (p-ERK) binds at FLNA^{CT}. This interaction regulates endoplasmic reticulum and plasma membrane towards the contact sites. Interestingly, the deletion of *FLNA* results in F-actin cytoskeleton modification from homogeneous to cortical distribution, whereas the absence of p-ERK leads to more enrichment of FLNA in plasma membrane [30]. In our previous studies, we have observed a decrease in lung tumor size in an *Flna*-deficient mouse model, despite the constitutive expression of KRAS. Our *in-vitro* studies indicated that *Flna*-deficient KRAS-transformed fibroblasts proliferate and migrate poorly. These cells also express lower phosphorylated levels of both AKT

and ERK1/2 [31]. We also observed similar results in mice that are deficient in FLNA specifically in endothelial cells. In these studies, both cell migration and the size of tumor xenografts are reduced, due to the absence of endothelial FLNA. *In-vitro* studies have also shown defects in endothelial cell migration that might be due to lower levels of p-AKT and p-ERK1/2 [31].

FLNA interaction with the SPHK1-interacting protein induces cell migration, lamellipodia formation and FLNA phosphorylation in A7 melanoma cells [32]. FLNA expression negatively regulates sphingosine-1-phosphate and NF- κ B activation in *FLNA*-deficient M2 melanoma cells [33]. In these cells, RelA (p65) is phosphorylated to a greater degree, resulting in the activation of NF- κ B protein. NF- κ B is regarded as the key regulator for many of the inflammatory responses [33]. FLNA also interacts with the ring zinc finger domain of tumor necrosis factor receptor-associated factor 2 (TRAF2). TRAF2 is thought to negatively suppress the activation of NF- κ B via the JNK/SAPK pathway [34]. When *FLNA* is epitopically overexpressed in *FLNA*-deficient M2 cells, TRAF2 is silenced and the JNK/SAPK pathway is induced, resulting in the activation of NF- κ B in M2 cells [34]. This suggests that FLNA controls various signaling pathways leading to inflammatory responses.

Filamin A in cellular migration

Cell migration is regarded as the crucial step during embryogenesis, wound healing and also pathological processes, such as immune

responses, tumor formation and metastasis. All these processes require the specific movement of particular cells to designated locations. Cell migration is a schematic process which is involved in cell polarization, protrusion in the direction of cell movement, retraction and release from the rear. FLNA is present in most motile cells at both the leading and rear end. FLNA has been shown to be involved in the remodeling of the actin cytoskeleton and cell protrusion and retraction.

FLNA is involved in the organization of actin filaments to the cell membranes, which helps to provide scaffolding for multiple cytoskeletal proteins by the integration of cell adhesion [3, 6]. The immunofluorescent staining of cultured cells indicates that FLNA is more localized to lamellipodia, filopodia, stress fibers and focal adhesions [35]. The possible suggested mechanisms behind these processes could be the specific binding partners of FLNA, such as receptors and adhesion molecules that mostly reside in the cell region under movement [36]. Another possible explanation could be higher concentrations of FLNA in newly assembled actin sites in lamellipodia, due to greater avidity for the branched F-actin junctions [9, 37].

FLNA is more concentrated towards adjacent sites to the cell membrane during cell spread [38] and subsequently towards adhesion sites when force is applied [39]. This indicates the importance of FLNA in regulating the strength of cell adhesions and the process of cell adhesion. FLNB is mostly associated with stress fibers and does not localize to focal adhesions like the FLNA isoform.

Since the discovery of FLNA in 1975, FLNA binding partners have been increasing at a steady pace and there are now more than 90 binding partners, in addition to an association with actin filaments [5]. The majority of the interacting partners play a significant role in regulating cell adhesion, migration and cell spread [40]. In the first case report on FLNA mutations, an association with periventricular nodular heterotopia (PVNH) was reported [41]. Subsequently, multiple studies have focused more heavily on *FLNA* function in neuronal migration, as mutations in *FLNA* prevent the migration of cortical neurons in PVNH. Interestingly, the overexpression of *FLNA* also prevents neuronal migration [25]. However, *Flna*-deficient mice do not develop PVNH and even the embryonic fibroblasts do not display any defects in cell migration and growth [18, 42]. This might be due to small brain volume, less complex than that in humans. However, these mouse embryos exhibit a thinner cerebral cortex, indicating defects in cell migration [18].

Interaction partners of filamin A

Integrins

The majority of the cells migrate in an integrin-dependent manner, even though certain cell types migrate in an integrin-independent manner without binding to integrin [43] and swim independently [44]. The relationship between the FLNA and integrins is mutual. When mechanical stress is conveyed by integrin β_1 , it recruits FLNA and F-actin towards focal adhesions which contain integrin β_1 [39]. FLNA is well situated in the cell, mediating the matrix-

cytoskeletal signaling with its dual binding capability. F-actin binds at FLNA^{NT}, whereas various transmembrane adhesion receptors and integrins bind at FLNA^{CT}. Integrin β_1 binds at Ig-repeats 16–24 of FLNA to regulate endothelial cell motility [45]. Integrin β_2 binding at repeat Ig-21 mediates leukocyte extravasation [46]. The binding of integrin β_3 at repeat Ig-21 promotes platelet aggregation. The binding of integrin β_7 at Ig-repeats 19–21 mediates lymphocyte migration [47].

Interestingly, FLNA has also been reported as a negative regulator of integrins. The depletion of FLNA reduces the cell surface expression of integrin β_1 . In *FLNA*-deficient cells, the cell surface expression of integrin β_1 is reduced during the initial 15 minutes of cell contact. Once *FLNA* expression is restored in these cells, integrin β_1 expression is rescued as well [48]. During mechanical stress, integrin β_1 recruits both F-actin and FLNA towards focal adhesions where integrin β_1 is present [49, 50]. Integrin β_1 also improves *FLNA* promoter activity and prolongs *FLNA* mRNA half-life by selectively activating the p38 pathway in fibroblasts [51]. In contrast, the inactivation of integrin β_1 function reduces *FLNA* expression in the localization and spread towards cell membranes. Reciprocally, the loss of *FLNA* function reduces the endogenous expression of integrin β_1 in human breast cancer cells [52], thereby increasing tumor invasiveness [53]. The silencing of *FLNA* increases calpain activity, leading to the turnover of focal adhesions, which may result in inducing tumor invasiveness [54, 55]. Furthermore, integrin

β_1 trafficking to the cell membrane is regulated by the PKC ϵ -mediated phosphorylation of vimentin [56], which is known to bind at Ig-repeats 1–8 of FLNA. The silencing of *FLNA* mRNA in culture cells impairs vimentin phosphorylation, leading to reduced cell adhesion and spread. This impaired cell spread is rescued by transfecting *FLNA*-deficient cells with Ig-repeats 1–8 alone, without complete ABD [56].

Even though the binding of FLNA to integrins is necessary for cell spread and migration, either too much or too little binding results in impaired migration and cell spread. Cell migration and adhesion are fine-tuning processes between two proteins and other integrin-binding partners.

GTPases

In mammalian cells, small GTPases regulate the generation of actin-based motile structures. Small GTPases are activated when integrins bind to the extracellular matrix, resulting in actin polymerization and the formation of lamellipodia and filopodia. Branched actin networks are the key ingredients in the formation of lamellipodia, which drive the cells to move forward. FLNA interacts with RalA and small GTPases, including Rho, Rac and Cdc42. FLNA interacts with the majority of the upstream- and downstream-signaling molecules of GTPases. The majority of interactions occur in the FLNA^{CT} region at Ig-repeats 23–24 [57]. In *FLNA*-deficient melanoma cells, RalA fails to generate filopodia and, when FLNA is reintroduced by transfection, filopodium has been generated in these cells.

This suggests that RalA may recruit FLNA to filopodium to regulate RalA-mediated filopodial protrusion [57]. FLNA interacts with PAK1, which in turn activates PAK1 and phosphorylates FLNA, as the activation of PAK1 is necessary for membrane ruffling [58]. Another pathway to activate PAK1 is by binding to sphingosine kinase 1. The interaction between FLNA and sphingosine kinase 1 activates a potent lipid mediator, sphingosine-1-phosphate, which directly activates PAK1 kinase activity [32]. PAK1 is a downstream effector for both Rac1 and Cdc42. FLNA also coordinates the Rac GEF trio [36] and Rho GEF Lbc [59]. This coordination supports the spatial positioning of actin assembly. FLNA interacts with FilGAP and this interaction may inactivate Rac and promote cell retraction by suppressing leading edge protrusion [60]. To summarize, FLNA anchors GTPase signaling to cell membrane proximity where it converts from GDP to GTP to provide scaffolding and coordinate actin remodeling activities.

Transcriptional factors

Recent studies indicate that FLNA is involved in transcriptional activity, either by regulating transcriptional activity by activating the transcriptional factors or by the repression of transcriptional factors by retaining them in the cytoplasm. The majority of transcriptional factor interactions take place in the FLNA^{CT} region. FLNA interacts with SMAD2 and SMAD5, positively inducing the receptor-induced phosphorylation of SMAD2 and SMAD5, as well as nuclear accumulation [61]. However, the interaction of FLNA with PEBP2 β /CBF β ,

the subunit of PEBP2/CBF transcriptional factors, inhibits the binding ability of this complex to RUNX1 [62] or binding to another transcriptional regulator, p73 [63]. This interaction represses transcriptional activity and retains it in the cytoplasm of human melanoma cells [63]. FLNA may also participate in the DNA damage-response pathways by interacting with the tumor suppressor gene, BRCA2, in HeLa cells [64]. It has previously been demonstrated that the transcriptional activity of FOXC1 is mediated by the interaction of FLNA with PBX1. PBX1 interacts with the full-length FLNA protein efficiently to transport PBX1 to the nucleus, where it forms a transcriptional inhibitory complex with FOXC1–PBX1 in A7 melanoma cells [65].

Recent studies indicate that FLNA is involved in the nuclear localization of transcriptional factors, but studies are still not complete. In androgen-dependent prostate cancer cells, FLNA is cleaved by calpains, producing a 90 kDA FLNA^{CT} fragment. It is then localized to the nucleus. However, in androgen-independent cells, FLNA remains in the cytoplasm and fails to be cleaved by calpains [66]. Consistent findings indicate that FLNA is cleaved by calpains, resulting in the production of FLNA^{CT}. This fragment is involved in the nuclear transportation of the androgen receptor (AR). Along with AR in the nucleus, FLNA^{CT} represses the transcriptional activity of AR by interfering with interdomains and the co-activator binding site of AR [27, 67]. FLNA interaction with transcriptional factors in general may thus promote cell movement by

inducing the expression of growth factors by either autocrine or paracrine signaling.

In our previous studies, we have reported a novel interaction between FLNA and the hypoxia-inducible factor-1 α (HIF-1 α). When mammalian cells are exposed to lower oxygen levels, HIF-1 α helps them to adapt to hypoxic conditions [68] by activating a varying network of target genes [69]. During normoxia, HIF-1 α protein is degraded by a tumor suppressor, protein von Hippel-Lindau, acting as an E3 ubiquitin ligase and hydroxylation near-proline residues [70]. During hypoxia, hydroxylation is inhibited, resulting in the stabilization of HIF-1 α , which then translocates into the nucleus and activates its target genes, including vascular endothelial growth factor-A (VEGF-A) [71]. We have reported that a cleaved FLNA^{CT} fragment promotes the transcriptional activity of HIF-1 α by facilitating nuclear translocation and induces the secretion of VEGF-A [72]. In our Study I, we observed lower serum levels of secreted VEGF-A in mice deficient in FLNA in endothelial cells after a myocardial infarction (MI). We have observed more scar tissue and an enlarged heart in these mice, which indicate *Flna* deficiency in endothelial cells which then fail to generate new blood vessels around the infarcted cardiac muscle. This could be one reason why the infarction size increases in mice deficient in *Flna* in endothelial cells.

FLNA has the potential to regulate transmembrane receptor expression, by interacting with transcriptional factors and altering the cell response to various external cellular signaling, including growth factors. In our previous studies, we have shown that

the expression of c-MET is upregulated by FLNA, partly by the transcriptional factor, SMAD2. FLNA binds to SMAD2 to transport it to the nucleus [61], which in turn activates c-MET activity by binding to its promoter and regulates the cellular response to hepatocyte-growth factor (HGF) [73]. Mature c-MET receptor is a heterodimeric protein consisting of a 45 kDa α -subunit which is linked to a 145 kDa β -subunit by disulfide bonds [74]. The binding of c-MET to HGF triggers multiple phosphorylation sites, two in the kinase domain (Tyr1234 and Tyr1235) and two at the docking site (Tyr1349 and Tyr1356) [74]. Multiple signaling molecules and adaptor proteins are recruited at the docking site after phosphorylation, resulting in the activation of signaling cascades and triggering various tumorigenic responses, such as scattering, invasion, proliferation and branching [75].

In Study II, we discovered a novel interaction between FLNA^{CT} and a signal transducer and activator of transcription 3 (STAT3). We hypothesized that FLNA may likely facilitate the nuclear phosphorylation of STAT3 to further activate the secretion of the inflammatory response cytokine, IL-6. The STAT family consists of seven members [76]. STAT3 was first discovered in 1993 in mammalian cells. The STAT3 protein consists of six domains (1, amino-terminus; 2, coiled coil domain; 3, DNA binding domain; 4, linker domain; 5, Src homology two domains; and 6, carboxyl-terminal transactivation domain). The deficiency of *STAT3* results in embryonic lethality due to severe malformations in the visceral endoderm [77], indicating that STAT3 plays a vital role in development. STAT3

activation is mainly dependent on phosphorylation at two sites, tyrosine 705 and serine 727, which reside in the C-terminus. In response to cytokines IL-5, IL-6 and IL-10 and the growth hormone, leptin, STAT3 phosphorylates the Tyr705 site and is then translocated into the nucleus where it acts as a transcriptional factor [78]. Phosphorylated STAT3 binds directly to the γ -interferon site in the DNA promoter regions in cooperation with nuclear factors [79, 80].

STAT3 is widely described as the crucial mediator, which controls cell adaptation in response to external stimuli in both inflammatory cells and non-inflammatory cells such as endothelial and smooth-muscle cells [81]. STAT3 activity might act as a key regulator in mediating angiogenesis after MI [82]. The tissue-specific deletion of STAT3 in cardiomyocytes reduces myocardial capillary density in mice [83]. STAT3 is more phosphorylated in the atherosclerotic plaques of *ApoE* knockout mice, indicating a crucial role for STAT3 during the pathogenesis of atherosclerosis [84]. Plasma from these mice exhibits higher concentrations of circulating IL-6 [85]. STAT3 considerably regulates the number of cytokines by regulating its transcription in macrophages and smooth-muscle cells [81]. Crosstalk between vascular smooth-muscle cells and monocytes elevates both IL-6 and STAT3 expression, resulting in the upregulation of multiple cytokines in monocytes and enhanced reactive oxygen species in vascular smooth-muscle cells. These may contribute to the development of atherosclerotic plaques [86, 87]. STAT3 signaling operates in the IL-13 pathway to mediate foam cell formation [85].

Calpains and calpain inhibitors

The hinge regions of FLNA (H1 and H2) are proteolyzed by Ca²⁺-dependent calpains. The cleavage of these regions produces 90 kDa FLNA^{CT} and 200 kDa FLNA^{NT} [15]. Calpains are cysteine proteases that are present in the majority of mammalian cells and a few bacteria. Calpain in mammalian cells generally presents as calcium-dependent cysteine proteases, which consist of 15 isoforms [88]. Among these 15 isoforms, calpain-1 and calpain-2 are widely distributed and are the most studied isoforms and they are often referred to as conventional calpains [89]. Calpains contain two subunits, a small 30 kDa calmodulin-like calcium-binding unit and a large 80 kDa papain protease-like unit [90].

Calpains participate in various cellular and physiologic activities, such as cytoskeletal remodeling [91], cell motility, [92], embryonic development [93], signal transduction pathways [94], apoptosis [95], the regulation of gene expression [96] and cell cycles [97].

Apart from physiologic events, calpains are also involved in numerous pathologic events, which has led to the discovery of calpain inhibitors and their potency in therapeutics. Calpain inhibitors are generally classified into two groups; non-peptide calpain inhibitors (5-azolones, carboxamides, dihydroxychalcones and α -mercaptoacrylates) and peptidomimetic calpain inhibitors (α -helical inhibitors,

epoxysuccinate-based inhibitor and calpeptin) [98].

Therapeutic uses of calpain inhibitors

Calpain inhibitors are used in various disorders, including ocular disorders. Calpain 1 inhibits retinal visual cell regeneration [99] and also acts as an anti-cataract agent [100]. It has also been shown that the specific inhibition of calpains shields arteries, hair, skin and kidneys from age-related lesions, as well as telomere shortening [98]. Calpain 1 is hyperactivated in Alzheimer's disease, due to a calcium overload in susceptible neurons, suggesting calpain 1 as a potential target for Alzheimer's disease [101]. Calpain 1 is negatively responsible for the regulation of erythrocyte deformability and filtration. As a result, the inhibition of calpain 1 has been proposed as a therapeutic approach to treat sickle cell disease [98]. Calpain 3 inhibition is beneficial in treating tibial muscular dystrophy. Either the overexpression or the inhibition of calpain 3 inhibits disease progression [102]. It has also been shown that the inhibition of calpain 1 inhibits tumor cell growth in colorectal cancer [98]. Both calpain 1 and calpain 2 are extremely abundant in the heart [103]. Despite the higher concentrations of calpains detected during ischemic and reperfusion injury [104], calpain inhibitors in cardiovascular diseases (CVD) have not been studied in detail.

Mouse models of filamin A deficiency

The discovery of *FLNA*-deficient melanoma cells has prompted huge interest in exploring the cellular functions and interacting partners of FLNA in far greater detail. Seven human melanoma cell lines have been identified, three of which express lower mRNA levels for *FLNA* [105]. All three *FLNA*-deficient cell lines exhibit the continued blebbing of plasma cell membrane, impaired pseudopod protrusion and cell motility. When *FLNA* deficiency has been restored in these cell lines by transfecting the full-length coding sequence of *FLNA*, cell migration has been normalized and they migrate five times faster than *FLNA*-deficient cells in response to a chemoattractant [105].

In 2006, two different *Flna*-deficient mouse models were developed, one which is chemically induced and another which is a genetically modified model. A nonsense mutation has been introduced in Ig-repeat 22 (Y2388X), designated as *Dilp2* in the chemically induced model, and it results in the loss of *Flna* function [42]. This mutation is induced by N-ethyl-N-nitrosourea, which results in the conversion of tyrosine to stop codon, causing lethality in males due to arterial trunk, midline fusion defects and palate abnormalities in males [42]. A genetically modified mouse has in fact been generated by introducing flox sites in the *Flna* gene between introns 2 and 7 in female mice. The crossbreeding of these female mice with β -actin Cre male mice results in earlier truncation at the 121 amino acid in the CH1

domain, causing embryonic lethality in males, with severe cardiovascular abnormalities and abnormal vascular patterning [18]. Surprisingly, none of these mouse models shows the PVNH phenotype, which might be due to a compensatory role for the *Flnb* isoform or else the mouse genome is not entirely similar to the human genome.

In the following years, more *Flna*-deficient mouse lines have been developed to study distinct roles for *Flna* in specific cell types. Mice that are deficient in *Flna*, specifically in smooth-muscle cells, have lower blood pressure, along with a decreased pulse rate, aortic dilation and an increase in atrial compliance [106]. Mice that are deficient in *Flna*, specifically in megakaryocyte cells, have severe macrothrombocytopenia due to accelerated platelet clearance, accompanied by lethality in late embryogenesis. The *Flna*-deficient megakaryocyte cells are prematurely large and have fragile platelets which are quickly cleared by macrophages in circulation [107]. Mice that are deficient in *Flna*, specifically in endothelial cells, show no abnormalities in vasculature or heart pump function, but, when myocardial infarction (MI) is induced in these mice, the endothelial cells in *Flna*-deficient mice fail to generate new blood vessels, which results in a larger infarction size. Nor do mice that are deficient in *Flna* in monocytes show any abnormalities. They are fertile and viable. However, *Flna*-deficient monocytes fail to develop multinucleated osteoclasts and poor monocyte migration, which might be controlled by Rho GTPase activation, indicating that *Flna* might be required in the

earlier stages of osteoclastogenesis [108]. In Study II, we deleted *Flna* in macrophages, similar to what is mentioned above, and we observed no phenotype in the mice, but, when atherosclerosis is induced as a result of a Western diet, mice deficient in FLNA in macrophages develop smaller plaques due to impaired macrophage cell migration, lipid uptake and cytokine response.

Myocardial infarction

MI is usually referred to as the death of the heart muscle, the myocardium. It is also usually referred to as a heart attack, but it is a different form, where the heart muscle is damaged due to reduced blood flow, resulting in cardiac arrest. This is an acute cardiovascular disorder caused by a short-term or sudden change in blood flow to the heart. MI was responsible for more than 15 million cases around the world in 2016 alone [109]. Smoking, diabetes, hypertension, reduced physical activity and obesity are some of the most important risk factors for MI. The symptoms include chest pain, shortness of breath, a sensation of tightness and radiating pain mostly in the left arm, but it can also affect other parts of the body. Other minor symptoms include sweating, nausea and fainting; however, about 5% of MI cases do not exhibit any of the symptoms.

Atherosclerosis is the main cause of MI due to the rupture of the plaque, blocking the artery and restricting blood circulation to the heart muscle [110]. The other factors which contribute to MI are limited oxygen demand or hypoxia conditions, hyperthyroidism and low blood pressure. The restriction or

blockage of the artery near the heart muscle triggers an ischemic cascade where the heart cells in the surrounding tissue die due to necrosis and cannot be regenerated [111]. The surrounding tissue cells affected by oxygen obstruction have to generate ATP in mitochondria. This mechanism triggers necrosis and apoptosis in the affected cells [111]. The innermost tissue, the endocardium, is the most susceptible layer during damage, as ischemia is a first trigger here. The cells surrounding tissue begin to die within 15-30 minutes of obstruction and the first wave of muscle damage usually begins in three to four hours [111, 112]. The size and location of the infarct often determines the risk of heart abnormalities known as arrhythmias, aneurysms, inflammation in the heart wall and rupture [112].

An MI is mostly diagnosed by elevated levels of troponins which are usually released after four to eight hours and peak after one to two days of muscle damage [113]. A change in heart pump function and motion is detected by an echocardiogram, while thrombus formation is detected by an angiogram.

Endothelial cells in myocardial infarction

Endothelial cells are crucial for the formation of angiogenesis and vasculogenesis. The entire circulatory system from the heart to the smallest capillaries is covered in vascular endothelial cells. They are responsible for a wide range of functions, such as fluid filtration, blood vessel tone, hemostasis, neutrophil recruitment and hormone trafficking. The entire vascular system is

lined by a single layer of endothelial cells. The endothelium alone comprises of 1×10^{13} cells in adults, almost equivalent to 1 kg of an organ [114]. The main function of endothelial cells is to maintain the structure and functional integrity of the vessel wall. They also act as a semi-permeable barrier regulating the transfer of small and large molecules [114]. When a person suffers an MI, the left ventricle undergoes dramatic changes at both the cellular and functional level of the heart [115]. Pro-angiogenic therapy has been long regarded as promising treatment, where vascular endothelial cells are induced to migrate to surround damaged heart tissue and promote angiogenesis to generate new blood vessels. Pro-angiogenic treatments have not been established, despite numerous efforts in hypoxia-induced angiogenesis. As a result, further detailed studies have to be performed on mechanisms dealing with vascular endothelial cells to prevent MI. FLNA has long been thought to be involved in cellular migration and angiogenesis and the loss of *FLNA* results in PVNH, accompanied by other cardiovascular phenotypes in humans. The loss of *Flna* function in the mouse is accompanied by embryonic lethality caused by severe cardiac malformations and abnormal vascular patterning [18]. So, in Study I, we studied the role of the vascular endothelial-specific expression of FLNA post MI by deleting *Flna* in endothelial cells.

Atherosclerosis

Atherosclerosis is a chronic inflammatory disease and it is involved in every stage of CVD [116, 117]. Atherosclerosis is generally

classified by the build-up of plaque and the formation of fatty streaks in the arteries [118]. It is a major cause of death in the USA, Europe and a few parts of Asia. In Sweden, around one million people suffer from CVD and most of these cases are atherosclerosis related. The progression of atherosclerosis disease is based on two hypotheses; during its early phase, by the initial response of the inflammatory cascade to endothelial dysfunction, followed by the retention of low-density lipoproteins (LDL) in the wall of arteries [119], while the other hypothesis is that the lipids come first and are followed by endothelial injury, which is supported by the presence of fatty streaks in the absence of inflammation [120, 121]. Even though atherosclerosis has a high mortality rate, the progression of the disease is still debatable. However, the most widely accepted theory is systemic inflammation during the progression of atherosclerosis. Regardless of which hypothesis comes first, elevated levels of lipids are responsible for most of the disease progression, followed by hypertension, diabetes, oxidative stress and viral infections [122]. Atherosclerosis generally remains asymptomatic until the age of 40 or 50 years, after which it becomes a major cause of death in Western countries. So, a better understanding of disease progression may give us clues to how cell signaling and cytokine production are regulated.

Macrophages in atherosclerosis

Macrophages are generally phagocytic cells and execute immune properties as they engulf and digest all foreign materials in body [123] and play a vital role in

atherosclerosis. The macrophage is a white blood cell that exists in various tissues such as Kupffer cells, alveolar macrophages, microglia and osteoclasts. Nevertheless, its function remains same; the phagocytosis of different foreign or unwanted particles. Macrophages act as both inflammatory and anti-inflammatory cells by secreting a number of different cytokines and growth factors [123]. Along with foreign materials, macrophages also engulf fatty deposits and form foam cells in the blood vessel wall [124]. The formation of foam cells and thereby the build-up of plaque results in either the rupture of plaque or the narrowing of blood vessels, resulting in the blockage of the oxygen supply to the heart and other vital organs. This results in severe complications such as stroke and cardiac and renal failure [125]. Generally, atherosclerotic lesions comprise early and late lesions. Early lesions are usually clinically silent; the lesions start to grow from small deposits of intracellular lipids into extracellular lipid pools, whereas late lesions grow from an extracellular lipid core to surface defects including ulceration, thrombosis, rupture and hemorrhage [125]. *FLNA* is involved in both cellular migration and the induction of the inflammatory cascade by interacting with multiple signaling molecules. In Study II, we hypothesized that a deficiency in *FLNA* in macrophages reduces macrophage migration, lipid uptake and cytokine release *in vitro* and reduces atherosclerotic plaque formation in mice.

Human mutations in filamin A gene

Due to the versatile function of *FLNA* in cell migration and cell signaling, mutations of *FLNA* cause a varying range of developmental malformations which are even associated with cardiovascular disorders, whereas *FLNB* and *FLNC* mutations are mainly restricted to skeletal and cardiac muscle dysfunction. Since these proteins are a recent entry in the research field, their more predominant functions are yet to be discovered.

The first discovered mutation in the *FLNA* gene is the null mutation where coding amino acids are converted to a stop codon in exon 3, resulting in PVNH, where a six-layer neocortex is not formed due to failed neuronal migration [41]. PVNH is mainly linked to females, while the majority of hemizygous males are confined to embryonic lethality and liveborn males display aortic dilation and die from massive hemorrhage in the neonatal period [41]. Female patients with PVNH run a huge risk of strokes and are associated with other cardiovascular abnormalities like valvular abnormalities, persistent ductus arteriosus and aneurysms in the aorta [41]. A cluster of missense mutations resulting in substitutions of ABD have been identified, mainly in the Ig-repeats of 9, 10, 14, 16, 22 and 23 of *FLNA* [126]. These missense mutations are discovered in the otopalatodigital syndrome, Melnick-Needles syndrome and front metaphyseal dysplasia [127]. They are also accompanied by cardiac, tracheobronchial and urological

malformations, resulting in perinatal death [127]. However, phenotypes caused by the otopalatodigital syndrome, Melnick-Needles syndrome and front metaphyseal dysplasia are very distinct from PVNH [128].

The genomic deletion of codons for exon 19 that results in X-linked myxoid valvular dystrophies (XVMD) in the heart, a specific cardiovascular malformation [129]. XVMD are frequently involved in anomalies of the vasculature, which includes mitral valve prolapse, as well as mitral and aortic regurgitation. It is known that a defective signaling cascade in TGF- β results in

impaired mitral valve remodeling and FLNA contributes to changes in cardiac valves by regulating the TGF- β signaling cascade via interaction with SMADs [61]. XVMD are not linked with PVNH and other congenital disorders mentioned above. Exon 21 nonsense mutations, frameshift and 4-shift mutations have been identified in *FLNA* to cause bilateral PVNH, along with Ehlers-Danlos syndrome, accompanied by minor cardiovascular malformations [130]. A variant of PVNH associated with *FLNA* mutations and Ehlers-Danlos syndrome leads to the development of aortic dilation during early childhood [131].

Aims

Our previous studies indicated that FLNA regulates cell migration in both organ development and tumor progression. A deficiency of FLNA results in impaired oncogenic angiogenesis and tumor cell signaling. In this thesis, we determine the biological importance of FLNA in adaptive angiogenesis during cardiovascular remodeling.

Specific aims

We hypothesized that the absence of FLNA in endothelial cells impairs endothelial cell function and signaling and thereby worsens remodeling after myocardial infarction.

We hypothesized that the absence of FLNA and the inhibition of FLNA^{CT} produced by calpain cleavage in macrophages impair cytokine secretion, lipid uptake and thereby reduce atherosclerotic plaque size.

Methods

Histology and image analysis

In Study I, mouse hearts were extracted after arresting them in a diastolic state following the injection of 30 mM KCl intracardially. They were then processed with standard histology for further analysis. The hearts were sectioned at five different levels, 1 mm between each level, starting from the apex, and stained for Mason's trichrome to determine the infarction size between the groups. Images of the stained heart sections were captured using a Mirax scanner and the infarction size was quantified by Biopix software, as described earlier [31].

In Study I, human infarcted hearts and mouse infarcted hearts were paraffin embedded and sectioned at 6 μm and stained for hematoxylin and eosin (H&E). In Study II, human carotid endarterectomies and mouse aortas were paraffin embedded and sectioned at 6 μm , starting 2 mm from the aortic arch, and stained for H&E, as described earlier [132].

In Study I, paraffin-embedded human infarcted and mouse infarcted hearts were sectioned at 6 μm and stained immunohistochemically with antibodies against FLNA (Chemicon International), FLNB (Chemicon international) and FLNC (Kinasource), as described earlier [133]. In infarcted and non-infarcted regions of mouse hearts, a number of endothelial positive capillaries and replicating cells were stained immunofluorescently with CD31 (Thermo Scientific) and Ki67 (Thermo Scientific)

respectively, from at least seven mice in each group. Images were captured using a Leica Microsystems microscope. CD31-positive structures were counted manually and the Ki67 staining intensity was quantified using Biopix software, as described earlier [134].

In Study II, we stained advanced (type VI) and intermediate (type III) atherosclerotic plaques, obtained from a human carotid endarterectomy biobank provided by the Göteborg Atheroma Study Group (GASG), as characterized histopathologically earlier [135]. These paraffin-embedded sections were immunofluorescently stained using primary antibody CD68 recognizing macrophages (DAKO), FLNA (Bethyl Laboratories), smooth muscle-specific α -actin (Sigma Aldrich) recognizing vascular smooth-muscle cells and CD31 (DAKO) recognizing endothelial cells. DAPI was included for nuclear staining. Appropriate Alexa anti-rabbit and Alexa anti-mouse (Jackson ImmunoResearch) were used as secondary antibodies, as described earlier [136].

Conditional gene knockout strategy

All the mice used in these studies had a C57BL/6 background. In Study I, female mice expressing homozygously floxed sites flanked between exon 2–7 in the *Flna* gene (*Flna^{fl/fl}*) were crossbred with male mice heterozygously expressing Cre under the control of vascular endothelial cell-specific cadherin promoter (*VECadCre+*) (Figure 2).

This type of Cre murine line is the model mostly common and widely used to target gene expression specifically in vascular endothelial cells [137]. In Study II, female mice expressing homozygously floxed sites of *Flna* (*Flna^{fl/fl}*) were crossbred with male mice homozygously expressing Cre under the control of monocyte/macrophage-specific lysozyme-M promoter (LC). This type of Cre murine line is the model most commonly

used to delete gene expression in macrophages [138]. Experimental mice were selected by PCR genotyping for the presence of the *Flna^{o/fl}* allele and *Cre* (Figure 2), as described earlier [31].

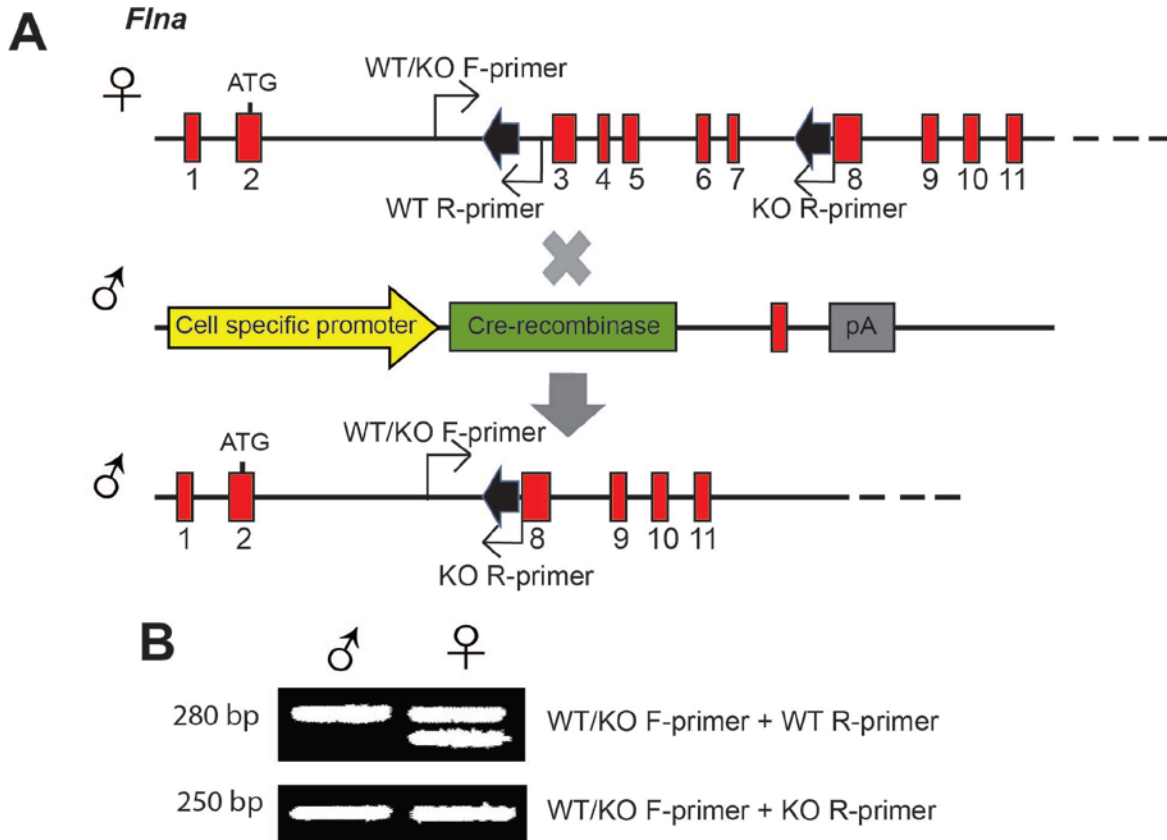


Figure 2. Cell-specific deletion of *filamin A* in mice. (A) Schematic illustration of the Cre-loxP system, where the floxed *Flna* gene is recognized by Cre recombinase, resulting in the deletion of *Flna* between 2–7 exons. (B) Confirmation of the presence of flox sites and the deletion of the *Flna* gene by PCR analysis.

Cell culture

Endothelial cells

In Study I, mouse primary endothelial cells were isolated from both mouse heart and lung. The tissues were dissected into very fine pieces and passed through a cell strainer until a single cell suspension was achieved. The cell suspension was incubated with Dynabeads (M-450, sheep anti-rat IgG, Invitrogen) coated with rat anti-ICAM2 (BD Biosciences). The endothelial cell-bound beads were washed with RPMI medium, along with growth factors, and plated on collagen II-coated culture dishes, as described earlier [31].

To study the expression of signaling molecules after silencing for *FLNA*, transformed mouse pancreatic endothelial MS1 (ATCC) was cultured in normal DMEM growth medium in Study I, as described earlier [133]. To study the tube formation assay, human umbilical vein endothelial cells (HUVEC) were cultured in basal medium supplemented with growth factors (EBM-2 bullet kit LONZA), as described earlier [134].

Macrophages

Primary macrophages were isolated from bone marrow of either control or experimental mice. Murine bone marrow was collected from the tibia and femurs and lysed using red blood cell lysis. Lysed bone marrow was then re-suspended in RPMI medium, along with mouse cardiomyocyte growth medium (CMG) as a source of M-CSF supernatant. To transform monocytes into macrophages, 10–15 million cells were

plated on 15 cm plates and cultured for at least seven days, along with CMG.

Human primary macrophages were isolated from peripheral donor blood and cultured with M-CSF for five days before experiments, as described earlier [139]. Human THP1 cells were supplemented with 100 nm of PMA to transform cultured monocytes into macrophages, as described earlier [132].

Cells assays

Migration

Wild-type (*wt*)- and *Flna*-deficient endothelial cells (Study I) and macrophages (Study II) were seeded in 8 μ m Boyden chamber inserts and cultured for 8-12 hours. Migrated cells were fixed and stained and the number of migrated cells was counted, as described earlier [31].

Proliferation

In Study II, *wt*- and *Flna*-deficient macrophages were seeded in six-well plates and cultured for up to five days. The total number of cells was counted every day and the average number of proliferated cells was plotted between the groups.

Cell shape assay

To determine the morphology of the cells, we stained *wt*-, *Flna*-deficient and MS1 endothelial cells for actin filaments (Study I) and mouse primary macrophages (Study II) with Alexa flour Phalloidin 488 (Life Technologies) and the nucleus with DAPI, as described earlier [140]. Images were captured using a Zeiss microscope.

Tube formation assay

In Study I, HUVEC cells transfected with scrambled control or *FLNA* siRNA were assayed on Matrigel-coated chamber slides overnight. The images were captured using a Zeiss microscope and the total number of formed tubes and the individual length of each tube formed between the groups were quantified using Image J software, as described earlier [140].

Foam cell formation and cholesterol efflux assay

In Study II, *wt*- and *Flna*-deficient and *FLNA*-silenced mouse and human primary macrophages were incubated with 50 µg/mL of minimally oxidized LDL (mmLDL, Kalen Biomedical) to measure the intracellularly accumulated level of mmLDL within 24 hours. Macrophages were then stained with an Oil-red-O stain and the nucleus was stained with hematoxylin to determine the accumulated lipids. Four random images were captured from each well using Leica Microsystems and the total accumulated lipids were quantified using Biopix software.

For lipid uptake assay, *wt*- and *Flna*-deficient macrophages were incubated with fluorescently labeled, either Dil-labeled total LDL or OxLDL (Invitrogen), for three hours. Four random images were captured from each well using Leica Microsystems and fluorescence intensity was analyzed using Biopix software, as described earlier [132].

To study the levels of excreted cholesterol, 5 x 10⁵ *wt*- or *Flna*-deficient macrophages were seeded in 24-well plates and incubated with 50 µg/mL of acetylated LDL (AcLDL)

and 5 µCi/mL of ³H-labeled cholesterol (Perkin Elmer) for 24 hours. These macrophages were rested overnight and treated separately with 20 µg/mL of HDL (Calbiochem) or 20 µg/mL of ApoAI (Sigma Aldrich) as the cholesterol acceptor for 12 hours. The levels of excreted ³H-labeled cholesterol in the cell culture medium were then measured using a scintillation counter. The results were normalized to protein concentration, as described earlier [132].

Silencing mRNA expression of filamin A

MS1, HUVEC cells (Study I), human primary macrophages and THP1 (Study II) were transfected with control siRNA or siRNA *FLNA* (5'-TACAGGCAATATGGTGAAGAA-3') and shRNA control or shRNA *FLNA* (5'GGAGTGCTATGTACAGAAAT-3), according to the manufacturer's protocol (Life Technologies). The efficiency of *FLNA* silencing was confirmed by either immunoblotting or real-time PCR.

Real-time PCR

Total mRNA was synthesized from both *wt*- and *FLNA*-deficient endothelial cells, HUVEC and MS1 cells (Study I) and human primary macrophages and THP1 cells (Study II). Total mRNA was synthesized to cDNA (Quanta Biosciences kit). The efficiency of *FLNA* silencing was measured by (Mm01187533-m1) probes and normalized to *GAPDH*.

Immunoblotting

Proteins were isolated from *wt*- and *Flna*-deficient endothelial cells (Study I) and macrophages (Study II). Proteins were isolated using mammalian cell lysis buffer (Sigma Aldrich) and the protein concentration was measured using a BCA assay (Pierce). Primary antibodies directed against FLNA (Chemicon, Bethyl Laboratories and Novus Biologicals), p-STAT3 (Cell Signaling), total STAT3 (Cell Signaling), p-AKT, total AKT, p-ERK1/2, total ERK1/2 (Cell Signaling), SR-B1 (Santa Cruz Biotechnology), LXR α/β , CD36, COX2, ABCG1 and ABCA1 (Novus Biologicals) were used. The protein expression between the groups was analyzed by their densitometric readings using Quantity One 4.4 software (Bio-Rad) in at least quadruplicates, as described earlier [140]. Cells were stressed with either serum starvation overnight (Study I) or treated with 10 ng/ml lipopolysaccharide (LPS) for 15 minutes (Study II) before the isolation of proteins.

Nuclear and cytosolic protein extracts were separated using an extraction kit (Thermo Scientific) to study p-STAT3 in Study II. Tubulin served as a cytoplasmic loading control and histone served as a nuclear protein loading control.

For the co-immunoprecipitation assay, total cell lysates were immunoprecipitated using antibodies against either FLNA^{CT} or STAT3. Dynabeads were coupled with targeted antibody and antibody-bound beads were incubated with at least 1 mg of total protein overnight. These beads were washed and then

immunoblotted for either FLNA^{CT} or STAT3, according to the manufacturer's protocol (Thermo Scientific).

ELISA

In Study I, secreted levels of N-terminal prohormone of brain natriuretic peptide (NT-proBNP) (Bio Source) and VEGF-A (R&D Biosystems) were studied from mouse serum. In Study II, interleukins IL-6, IL-10 and IL-12 were detected from either mouse serum or cultured macrophage medium, as described earlier (eBiosciences). In Study II, macrophages were cultured in 96-well plates, along with LPS (10 ng/ml), for eight hours with or without the calpain inhibitor, calpeptin (80 μ M) or STAT3 inhibitor DPP 5,15 (60 μ M), and secreted cytokine levels were then detected from cultured medium, as described earlier [132].

Mouse model of myocardial infarction

As previously reported [134], 14 to 16-week-old control (*Flna*^{o/fl}) and experimental mice that are deficient in *Flna* in endothelial cells (*Flna*^{o/fl}/*VECadCre*⁺) were used for myocardial infarction (MI) surgery. The left anterior descending artery (LAD) was permanently ligated to induce MI. During the surgical procedure, the mice constantly inhaled 3% isoflurane and 30% oxygen. Buprenorphine at a concentration of 0.05% as an analgesic agent was administered intraperitoneally after surgery. An ultrasound was performed a week later to determine the size and location of ligation. After 25 weeks, a cardiac ultrasound was performed under 2% isoflurane to record cardiac parameters

such as echocardiography, the ejection fraction and lumen areas between the groups. For a stress test, dobutamine was administered intraperitoneally (1 µg/g mouse body weight). An ultrasound was performed after the administration of dobutamine at baseline, five and 15 minutes to study whether cardiac parameters were altered between the groups. The hearts were extracted after arresting them in a diastolic state following an intracardial injection of 30 mM of KCl and subsequently processed with histology for further analysis, as mentioned above.

Mouse model of atherosclerosis

Bone marrow transplantation

In Study II, 12-week-old *Ldlr*^{-/-} mice were irradiated by a lethal 9.5 Gy dose, as previously described [141]. Bone marrows were isolated from 10-12 weeks of age from either control mice (*Flna*^{o/fl}) or mice deficient in *Flna* in macrophages (*Flna*^{o/fl/LC}). Bone marrow was suspended in RPMI1640 without phenol red and two to four million cells per mouse were injected intravenously via the tail vein into *Ldlr*^{-/-} mice four hours after irradiation. A week after transplantation, these mice were fed a Western (high fat, high cholesterol) diet containing 1.25% cholesterol until 25 weeks.

Adenoviral infection of PCSK9 vector

In Study II, we induced atherosclerosis by infecting *Flna*^{o/fl} and *Flna*^{o/fl/LC} mice with 2x10¹¹ particles of adenoviral vector (Ad) overexpressing proprotein convertase subtilisin/kexin type 9 (PCSK9) injected intravenously, as described earlier [142].

These mice were fed a Western diet containing 1.25% cholesterol until 25 weeks.

In vivo calpeptin treatment

Following the induction of atherosclerosis by AdPCSK9, 8 to 10-week-old C57BL/6 mice were treated with or without calpeptin and then fed a Western diet for 20 weeks. The control mice were injected with DMSO dissolved in saline. Treatment with calpeptin was administered at a dose of 0.65 mg/kg dissolved in saline. DMSO and calpeptin were injected intraperitoneally three times weekly during the last eight weeks. After 20 weeks, aortas were isolated and stained with Sudan IV, as described below.

After 20-25 weeks of a Western diet, entire mouse aortas were isolated from the aortic arch to the iliac bifurcation. Aortas were fixed with 4% formaldehyde, pinned out under an inverted microscope and stained with Sudan IV. Stained aorta images were captured by an inverted Leica microscope and then analyzed by using Biopix software.

Statistics

All the graphs were plotted using GraphPad Prism 6 and either a two-tailed Student's *t* test or one-way ANOVA statistical analyses were performed between the experimental groups. All results were reported as means ± SEM values. A *P* value of less than 0.05 was considered significant. Regarding the analysis of the intensity of co-localized FLNA expression in macrophages present in intermediate and advanced plaques of human carotid endarterectomies, a test of Mander's overlap coefficients was applied.

Summary of results

Study I: Deficiency of filamin A in endothelial cells impairs left ventricular remodeling after myocardial infarction.

Recently, an increasing number of discoveries have shown that human *FLNA* mutations or a loss of function are associated with various cardiovascular abnormalities, such as valvular dystrophy, aortic dilation, patent duct arteriosus and cardiac valve disease [5]. This has prompted us to study the biological role of FLNA in endothelial cells, as these cells cover the inside of vessels and are involved in angiogenesis. Mice that are deficient in *Flna* in endothelial cells did not exhibit any differences in cardiac function parameters and no abnormality was observed in vascular patterning. However, tumors inoculated in these mice developed a smaller size compared with controls, probably due to poor endothelial cell function. These findings encouraged us to determine the role of the endothelial cell-specific expression of FLNA during the development and progression of MI, as the demand for endothelial response and signaling is very high.

We observed that mice that are deficient in *Flna* in endothelial cells displayed an enlargement and thinning of the left ventricle

wall, due to increased infarction size and impaired cardiac function following MI. Mice that are deficient in *Flna* in endothelial cells exhibited a larger infarction size (Figure 3A), impaired cardiac pump function (Figure 3B) and reduced capillarity, along with decreased left ventricle thickness (Figure 3C) and elevated NT-proBNP levels (Figure 3D). In the absence of FLNA in endothelial cells, we observed impaired tube formation, migration and signaling in endothelial cells. These results indicated that FLNA plays an important role in endothelial cell function and signaling, as a deficiency in FLNA in endothelial cells resulted in an increase in MI size and the development of cardiac failure. These new roles of FLNA provide new insights into the mechanisms behind cardiac remodeling and thus contribute to the development of new strategies to improve heart function after MI. In conclusion, the deletion of *Flna* in endothelial cells increases MI size, with attenuated cardiac parameters, due to a poor angiogenic response that is required for wound healing.

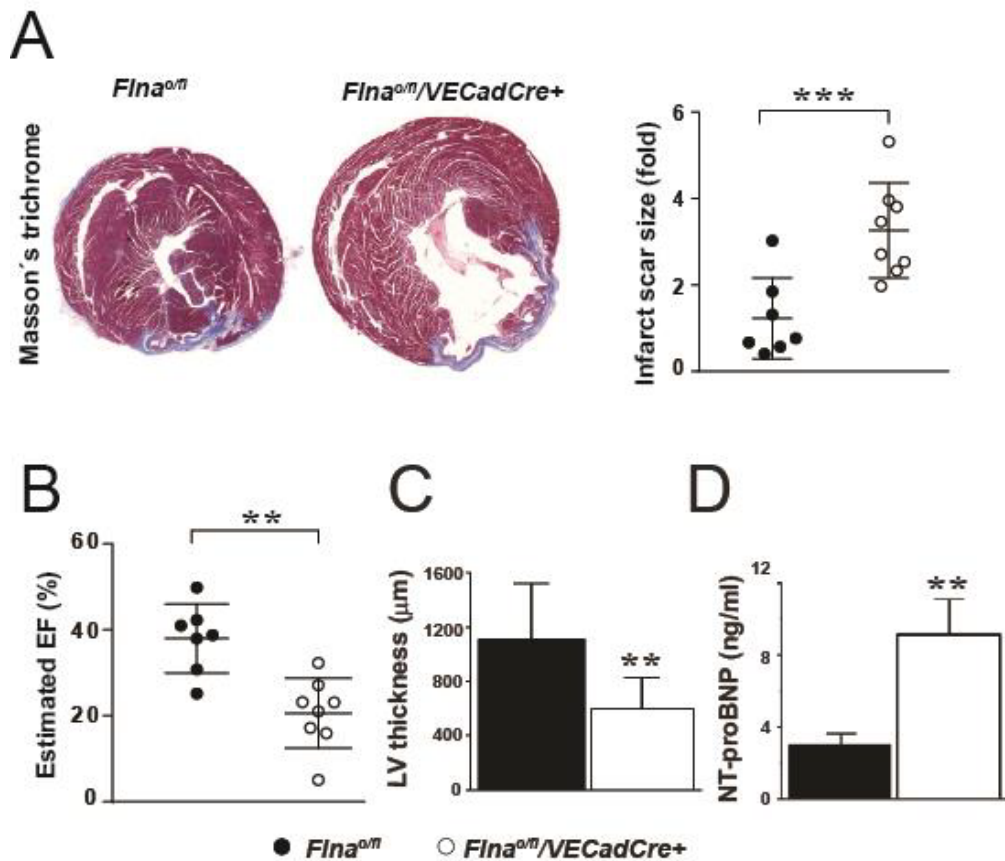


Figure 3. Increased size of MI and reduced cardiac function in hearts deficient in FLNA in endothelial cells. (A) Histomorphological changes in control hearts (*Flna^{o/fl}*) and hearts that are deficient in FLNA in endothelial cells (*Flna^{o/fl}/VECadCre+*) 25 weeks post MI, as detected by Masson's trichrome staining. Blue color represents the infarcted area, whereas red represents healthy non-infarcted myocardium (left panel). Image quantification of infarcted scar size (right panel). (B) Percentage of estimated ejection fraction between *Flna^{o/fl}* and *Flna^{o/fl}/VECadCre+*. (C) Measurement of histomorphological changes in left ventricular thickness. (D) Secreted serum levels of NT-proBNP, a biochemical marker of cardiac failure, 25 weeks post MI.

Study II: Targeting filamin A reduces macrophage function and atherosclerotic plaques in mice.

Atherosclerosis is a chronic disease with no cure to date. Understanding the molecular mechanisms in atherosclerotic disease progression will open doors to future curative treatment modalities. Macrophages play a key role in the progression of atherosclerotic plaques by taking up circulating lipids, forming foam cells and secreting inflammatory cytokines. FLNA regulates cell migration and proliferation in multiple cell types such as vascular endothelial cells and fibroblasts [31]. In this study, we hypothesized that macrophages that are deficient in *Flna* were able to migrate and proliferate less and this might then slow disease progression. To study this hypothesis, we deleted *Flna* in mice, specifically in mice macrophages, and induced atherosclerosis either by transplanting bone marrow that is deficient in FLNA in macrophages into atherogenic mice or by the overexpression of AdPCSK9 using an adenoviral vector and subjected mice to a Western diet for 20-25 weeks.

Macrophages without filamin A proliferate, migrate and secrete less IL-6

To determine whether FLNA has any effect on cell migration and/or lipid uptake in macrophages, we studied cell function by extracting primary macrophages from mouse bone marrow. *Flna* deficiency in these macrophages (*Flna^{o/fl}/LC*) resulted in impaired proliferation starting on day 4 (Figure 4A) and macrophage cell migration after eight hours (Figure 4B), as compared with *wt*-control macrophages (*Flna^{o/fl}*).

Subsequently, we studied atherogenesis *in vivo* by transplanting bone marrow from either control (*Ldlr^{-/-}* BMT: *Flna^{o/fl}*) or *Flna*-deficient mice (*Ldlr^{-/-}* BMT: *Flna^{o/fl}/LC*) into atherogenic *Ldlr^{-/-}*-deficient mice. These mice were subjected to a Western diet and their aortas were isolated after 25 weeks. The aortas were fixed, pinned and stained with Sudan IV to quantify fat plaques. Whole images of Sudan IV-stained aortas were captured and quantified using Biopix 9.2 image analysis software. We observed that atherogenic mice that received bone marrow deficient in FLNA in macrophages (*Ldlr^{-/-}* BMT: *Flna^{o/fl}/LC*) developed significantly (55%) less plaque compared with controls (*Ldlr^{-/-}* BMT: *Flna^{o/fl}*) (n = 11 and 13, respectively) (Figure 4C). To explain this decrease in atherosclerotic plaque size, we discovered that STAT3 interacts physically with FLNA^{CT} (Figure 4D). Nuclear levels of p-STAT3 were significantly reduced in *Flna^{o/fl}/LC* compared with *Flna^{o/fl}* macrophages. Furthermore, blocking the production of FLNA^{CT} by calpeptin significantly reduced nuclear p-STAT3 to levels similar to those of *Flna^{o/fl}/LC* macrophages (Figure 4E). Decreased levels of nuclear p-STAT3 reduced the secretion of inflammatory cytokine IL-6 in both *Flna^{o/fl}/LC* macrophages treated with calpeptin as compared to *Flna^{o/fl}* (Figure 4E) macrophages, suggesting that FLNA^{CT} plays an important role in regulating IL-6 secretion by interacting with STAT3.

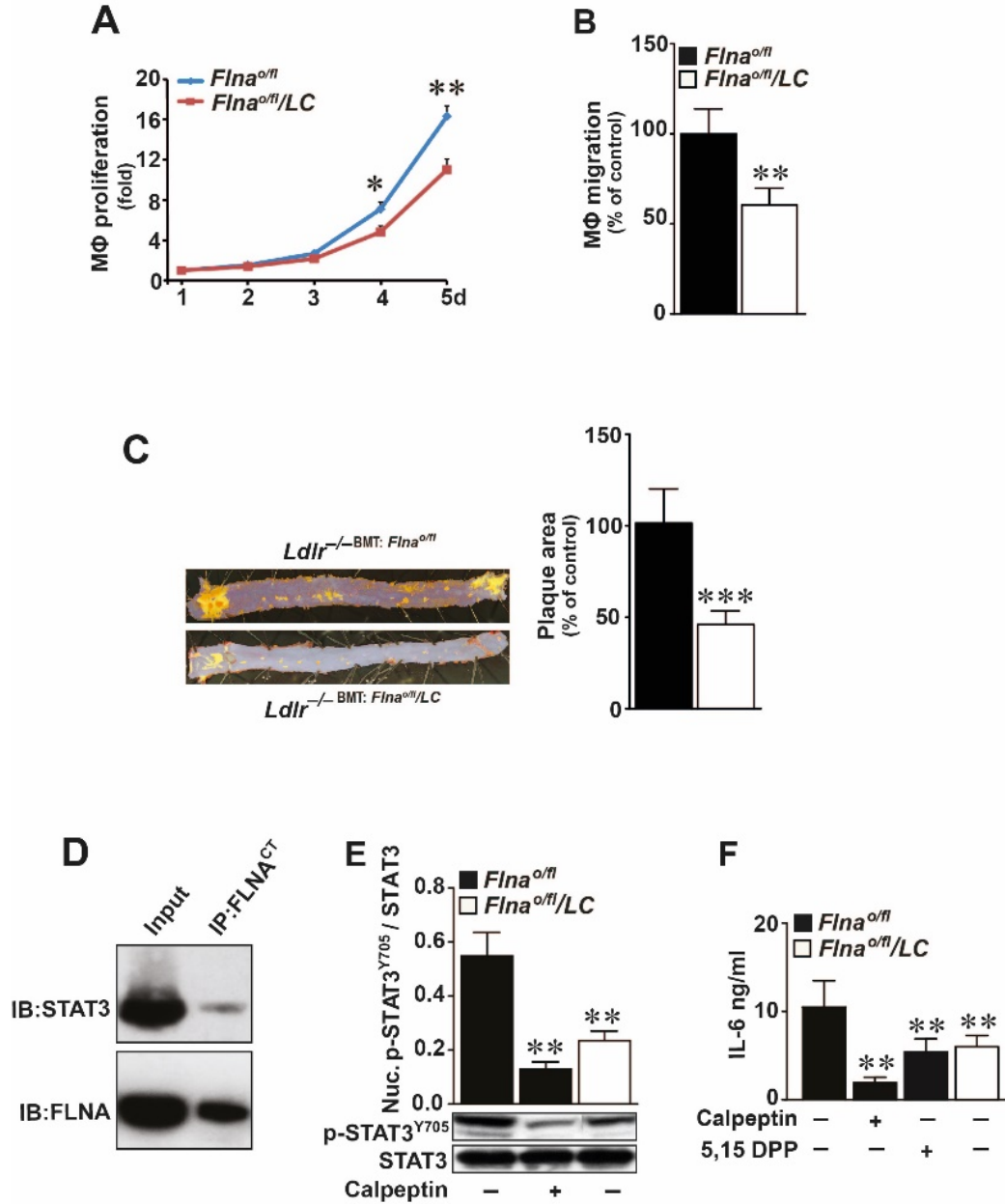


Figure 4. Impaired macrophage cell function and signaling in the absence of FLNA. (A) Number of proliferating *Flna^{o/fl}* and *Flna^{o/fl}/LC* macrophages up to five days. (B) Number of migrated *Flna^{o/fl}* and *Flna^{o/fl}/LC* macrophages after eight hours. (C) Images from Sudan IV-stained aortas obtained from *Ldlr^{-/-}* mice receiving either *Flna^{o/fl}* or *Flna^{o/fl}/LC* bone marrow (right panel). Percentage of plaque areas as quantified by image analysis of *Ldlr^{-/-} BMT: Flna^{o/fl}* or *Ldlr^{-/-} BMT: Flna^{o/fl}/LC* aortas (left panel). (D) Co-immunoprecipitation between FLNA^{CT} and STAT3 indicates that STAT3 is an interacting partner of FLNA^{CT}. (E) Quantification of nuclear levels of p-STAT3^{Y705} between *Flna^{o/fl}*, *Flna^{o/fl}/LC* and calpeptin-treated macrophages. (F) Secreted levels of IL-6 between *Flna^{o/fl}*, *Flna^{o/fl}/LC* and calpeptin-treated macrophages as detected by ELISA.

Filamin A-deficient macrophages take up lipids poorly

We then investigated whether *Flna* deficiency has any effect on foam cell formation and the uptake of lipids in macrophages, possibly explaining the lower plaque in *Ldlr*^{-/-} BMT: *Flna*^{o/fl}/LC aortas. *Flna*^{o/fl}/LC macrophages formed a significantly reduced number of foam cells. Similarly, we observed reduced foam cell formation in calpeptin-treated macrophages, as well as the specific inhibition of STAT3 signaling by 5,15 DPP-treated macrophages compared with control *Flna*^{o/fl} macrophages (Figure 5A). Oxidized lipids were also taken up poorly in both *Flna*^{o/fl}/LC and calpeptin-treated macrophages as compared with control *Flna*^{o/fl} macrophages (Figure 5B). We further investigated whether blocking the production of FLNACT alters macrophage cell proliferation and migration after treatment with calpeptin. This treatment

completely inhibited macrophage proliferation (Figure 5C) and partly blocked macrophage migration *in vitro* (Figure 5D).

Calpeptin treatment reduces plaque formation in mice

Based on our *in-vitro* results from calpeptin treatment, we initiated studies to determine whether calpeptin was able to inhibit atherogenesis *in vivo*. To achieve this, we induced atherosclerosis in eight- to 10-week-old C57BL/6 mice by infection with AdPCSK9. These mice were fed a Western diet for 20 weeks and treated with calpeptin at a dose of 0.65 mg/kg three times a week intraperitoneally for the last eight weeks. Aortas were pinned and stained for the presence of fatty plaques and these plaques were quantified as described above. We observed that calpeptin-treated aortas displayed areas of plaque that were significantly reduced by 49% as compared with control aortas (Figure 5E).

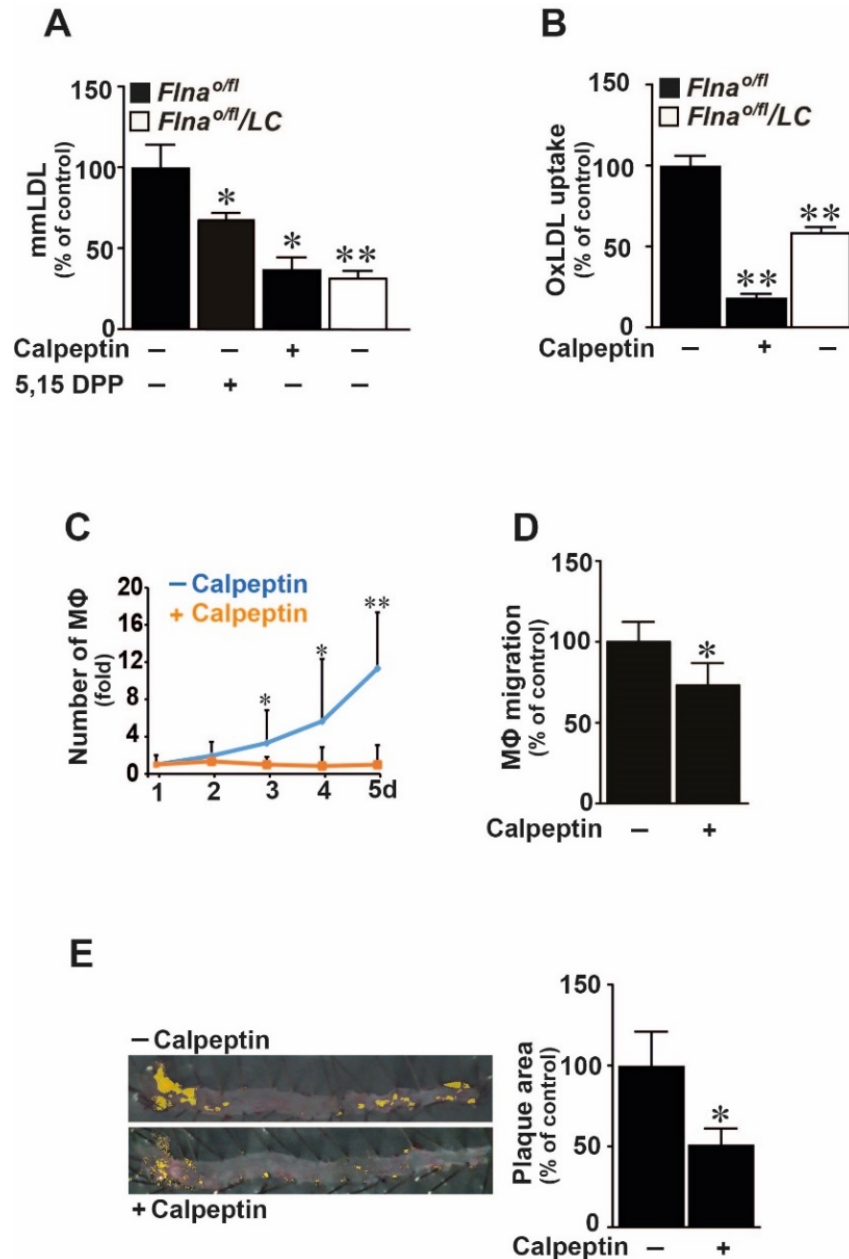


Figure 5. Treatment with calpeptin impairs macrophage function and reduces the size of atherosclerotic plaques. (A) Quantification of total accumulated minimally modified lipids in macrophages between the *Flna*^{off}, *Flna*^{off}/LC, calpeptin and a STAT3 inhibitor 5,15 DPP treatment groups after 24 hours. (B) Quantification of oxidized lipid uptake in macrophages between *Flna*^{off}, *Flna*^{off}/LC and calpeptin treatment groups after three hours. (C) Fold changes in the number of proliferating macrophages between groups treated with or without calpeptin up to five days. (D) Number of migrated macrophages between groups treated with or without calpeptin after eight hours. (E). Images from Sudan IV-stained aortas obtained from C57BL/6 mice infected with AdPCSK9, treated with or without calpeptin (right panel). Percentages of plaque area quantification by image analysis (left panel).

Discussion

Recent data indicate that, in addition to its cytoskeletal function, FLNA performs multiple functions in cellular signaling and transcription. In the studies in this thesis, we reported novel functions of FLNA during cardiovascular remodeling after MI and atherosclerosis. In the absence of FLNA in endothelial cells, the infarction size after MI was increased, probably due to impaired endothelial cell function and signaling. In the absence of FLNA in macrophages, the size of atherosclerotic plaques was reduced due to impaired macrophage function and signaling. To understand these biological roles of FLNA, we cultured both murine and human cells assayed for multiple functions in the absence or presence of FLNA *in vitro*. We then produced mice lacking FLNA in specific vascular cells to study cardiovascular remodeling.

An increased infarction size can be explained by three major factors. First, the absence of FLNA in endothelial cells resulted in impaired LV remodeling accompanied by increased infarction size and a thinned and enlarged LV wall after MI. Second, a reduced number of capillaries were observed in the peri-infarcted areas. Third, endothelial cells deficient in *Flna* displayed impaired cellular signaling, resulting in reduced migration and tube formation. Cardiac parameters were not altered in response to dobutamine stress in mice deficient in *Flna* in endothelial cells. Furthermore, the serum levels of NT-proBNP were higher in these mice, indicating an increased ventricular response to volume

expansion and possibly increased wall stress as a marker of heart failure.

The innermost layer of heart chambers is called the endocardium and it is covered by endothelial cells. The regenerating capability of cardiomyocytes is very limited and advanced atherosclerotic plaques reduce blood circulation in areas with cardiomyocytes requiring nutrients. To support cardiomyocytes in MI, endothelial cells are essential in the formation of new vessels by active migration and proliferation. Interestingly, we only observed a reduced number of capillary structures in infarcted areas. However, the number of capillary structures in non-infarcted areas remained unchanged. This suggests that angiogenesis regulated by FLNA was induced when these mice were exposed to a stressed condition. In the absence of stress, these mice did not exhibit any phenotype. We have shown no difference in endothelial cell proliferation, in contrast to fibroblasts and multiple cancer cell lines, in which the absence of FLNA reduces cellular proliferation. However, impaired endothelial cell migration *in vitro* in *Flna* deficiency may explain the increased size of MI in these mice. VEGF-A plays a dominant role in regulating angiogenesis during MI [143]. VEGF-A binds to VEGF receptor 2 to regulate downstream signaling molecules, including AKT, ERK and RAC-1 GTPase, during angiogenesis [144]. From our previous findings, we report that FLNA^{CT} interacts with HIF-1 α and regulates VEGF-A under hypoxia in human multiple cancer cells [72]. Interestingly, serum levels

of VEGF-A were decreased in mice deficient in *Flna* in endothelial cells after MI. The phosphorylation of kinases such as AKT and ERK1/2 and the level of active GTPase RAC1 were also reduced in cultured endothelial cells in the absence of FLNA (Figure 6). It is known that FLNA induces cellular migration either by direct interaction with RAC1 [108] or by the indirect regulation of VEGF-A [72]. In our studies, the absence

of FLNA in endothelial cells increases the size of LV, decreases cardiac pump function and leads to the development of cardiac failure by blunting angiogenic responses that are required for satisfactory wound healing. Inducing cellular signaling pathways regulated by FLNA and related to angiogenesis during MI could be a new approach to reduce the size of an MI.

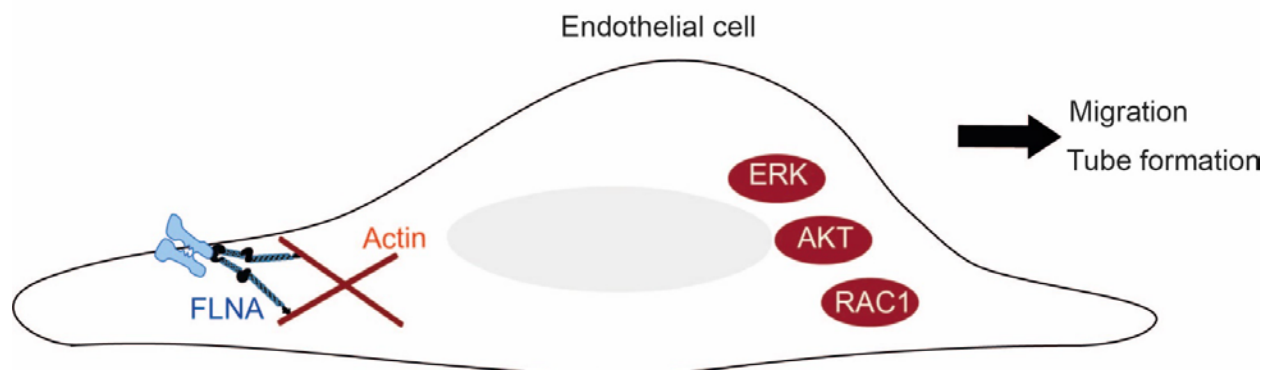


Figure 6. Schematic illustration of a proposed role for FLNA in endothelial cells. The expression of ERK1/2 and AKT and RAC1 activation are induced by FLNA during endothelial cell migration and tube formation.

In the progression of atherosclerosis, macrophage proliferation, migration, foam cell formation and an inflammatory response are the main events [145]. In our study, we have shown that the size of atherosclerotic plaques in atherogenic *Ldlr*^{-/-} mice receiving BMT deficient in *Flna* in macrophages was reduced. In addition, mice deficient in *Flna* in macrophages after overexpressing PCSK9 by an adenoviral vector displayed atherosclerotic plaques with a reduced size. We hypothesized that this plaque reduction could be based on three major findings. First, *Flna*-deficient macrophages secrete lower levels of the pro-inflammatory cytokines, IL-6 and IL-12, which could be partly regulated by STAT3 (Figure 7). Second, *Flna*-deficient macrophages proliferate and migrate less. Third, *Flna*-deficient macrophages take up fewer lipids and excrete more cholesterol as compared with *wt*-macrophage controls. Together, these three factors could explain the reduced size of atherosclerotic plaque in atherogenic mice deficient in *Flna* in macrophages. Cell migration and proliferation are regarded as key aspects in the progression of numerous diseases. We observed a smaller number of macrophages in the plaques in mice deficient in *Flna* in macrophages. *In vitro*, macrophages without FLNA proliferated and migrated less. This could be partly due to lower p-AKT and p-ERK1/2 in the regulation of macrophage proliferation and migration, similar to the endothelial cells in Study I, as well as human melanoma cells [72].

In atherosclerosis, macrophages secrete inflammatory cytokines in response to external stimuli. Anti-inflammatory therapies

have long been thought to reduce atherosclerosis and the treatment of atherogenic *Ldlr*^{-/-} mice with antibodies against the IL-6 receptor reduced the size of atherosclerotic plaques [146]. We observed a reduction in the secretion of IL-6 and IL-12 in *Flna*-deficient macrophage cells, as well as in mice deficient in *Flna* in macrophages. It is known that STAT3 partly regulates IL-6 secretion by binding to its promoter region [147]. In our *in-vitro* studies, we discovered that the FLNA^{CT} produced by calpain cleavage interacts with STAT3 and this complex is translocated into the nucleus to regulate the expression of *IL6*. We next determined that a deficiency of *Flna* in macrophages inhibits the nuclear p-STAT3, as well as IL-6 secretion *in vitro*. Interestingly, blocking FLNA^{CT} production by calpeptin treatment reduced the levels of nuclear p-STAT3, followed by the secretion of IL-6 in *wt*-macrophage controls to levels similar to those detected in *Flna*-deficient macrophages. This suggests that the cleavage of FLNA by calpain is important for STAT3 signaling by increasing the nuclear levels of p-STAT3 and thereby increasing the inflammatory response by IL-6 in macrophages.

Lipid uptake and the excretion of lipids from macrophages are the main vascular events in the formation of atherosclerotic plaques. In our *in vitro* studies, we observed that *Flna*-deficient macrophages take up fewer lipids and excrete more cholesterol. To explain these functional changes, we studied molecules that are involved in the unloading of cholesterol from macrophages without FLNA and discovered higher expression

levels of CD36, SR-B1 and COX2 by immunoblotting. Similarly, the treatment of control macrophages with calpeptin reduced foam cell formation as well as lipid uptake. Furthermore, the systemic administration of calpeptin reduced the size of atherosclerotic plaques in atherosclerotic control mice to levels similar to those we observed in mice deficient in *Flna* in macrophages *in vivo*.

To summarize, either a deficiency of *Flna* in macrophages or blocking production of FLNA^{CT} by calpeptin reduced proliferation, migration, secretion of inflammatory

cytokines and the formation of foam cells *in vitro*. These inhibitory effects may partly explain the reduced size of atherosclerotic plaques *in vivo*. In this study, we discovered a causal link for FLNA-dependent macrophage cell function during atherogenesis. Targeting the cleavage of FLNA by calpains might be a potential strategy to reduce plaque formation in atherosclerosis by decreasing macrophage proliferation and migration, the secretion of inflammatory interleukins and foam cell formation.

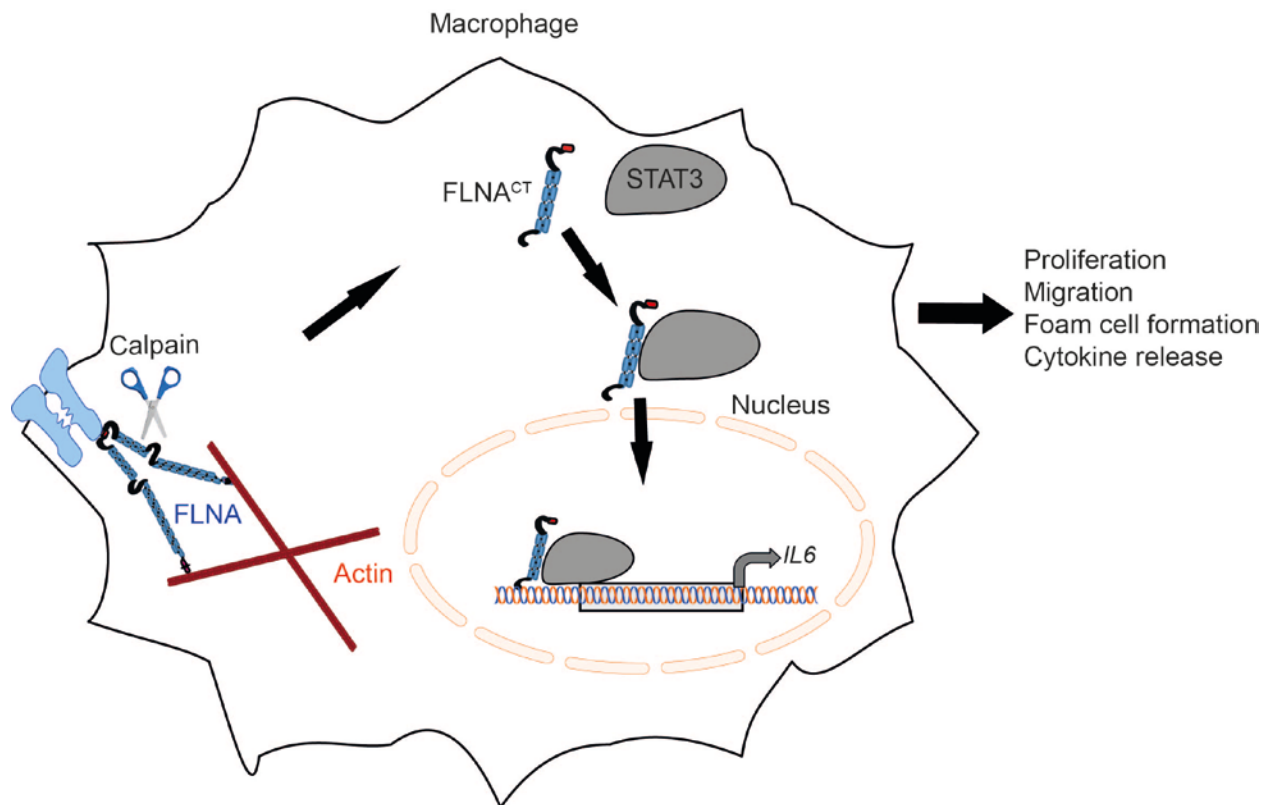


Figure 7. Schematic illustration of proposed mechanism between FLNA and STAT3 in macrophages. Cleaved C-terminal fragment of FLNA by calpain (FLNA^{CT}) interacts with STAT3 and this interacting complex is then translocated into the nucleus to regulate *IL6* gene expression.

Future directions

Filamin A as a prognostic marker

We identified FLNA as an important protein involved in atherogenesis. In order to suggest that FLNA has the potential to be used as a prognostic biomarker, the detailed expression of FLNA^{CT} needs to be detected in carotid endarterectomies. If the expression of FLNA^{CT} is increased, these patients may risk the development of severe clinical complications, such as new brain infarction events. Using cationic liposomes during percutaneous transluminal coronary angioplasty, FLNA may be overexpressed in coronary endothelial cells to promote angiogenesis in patients with MI.

FLNA is important during developmental stages and plays vital roles during embryogenesis, as a deficiency in *FLNA* is associated with lethality due to various severe malformations affecting the development of the heart, skeleton and brain in humans. Similarly, mice that are deficient in *Flna* die *in utero* due to severe cardiovascular malformations. Screening the presence and nature of *FLNA* mutations in humans and identifying the partner of *FLNA* that abolishes its binding capability in different mutated areas would be interesting in order to understand the biology behind the serious cardiovascular malformations. If critical *FLNA* mutations are identified, patients can be informed that they run a higher risk of developing cardiovascular malformations and can therefore be closely followed up by routine biochemical and radiological examinations.

Calpain inhibitors to treat atherosclerosis

Calpain inhibitors are widely used in various diseases, as mentioned above, but they have not been studied in detail in cardiovascular cells and disease remodeling. Calpain inhibitors have the potential to block the phosphorylation of FAK1, Src, Cdk5 and MAPK kinases that are involved in angiogenesis. In this thesis, we discovered a novel interaction by FLNA^{CT} with STAT3 in regulating the inflammatory signaling cascade that contributes to atherosclerotic plaque development. Blocking the production of FLNA^{CT} by calpeptin treatment impaired macrophage cell proliferation, migration, lipid uptake and nuclear p-STAT3 *in vitro*, as well as atherosclerotic plaque size *in vivo*. The systemic injection of calpeptin in mice did not produce any adverse effect on cardiovascular or liver histomorphology and ALT production. These results indicate that the inhibition of calpain might serve as a potential target to treat or at least slow atherogenesis.

Future experiments

As we discovered that the cleavage of FLNA by calpains is important for the nuclear presence of HIF-1 α and STAT3, we plan to mutate predicted sites of the H1 region cleaved by calpain and then generate the non-cleavable form of FLNA using a knock-in strategy using the CRISPR/Cas9 system in mice. Embryos expressing non-cleavable FLNA will be characterized for organ

development. If mice are born and survive normally, MI and atherosclerosis, as well as the growth of inoculated tumors, will be

investigated using models that we have already established in our laboratory.

Acknowledgements

This PhD thesis was mainly carried out at the *Institute of Biomedicine, Department of Medical Biochemistry and Cell Biology*, University of Gothenburg, Sahlgrenska Academy, between July 2014 and November 2018.

First and foremost, I would like to express my sincere gratitude to my supervisor, *Levent Akyürek*, for accepting me as a PhD fellow, for your continuous support during my PhD studies and research, for your motivation, enthusiasm and immense knowledge. Your patience and contribution in developing me as a scientist is irreplaceable and without you I cannot imagine where I would be as a person. Thanks for enormously stimulating discussions not only in science but also in life and career and always letting me choose the right path. Your guidance has helped me throughout my research and the completion of this thesis. I could not imagine having a better mentor than you during my PhD.

Previous and present members at the *Laboratory of Akyürek*. I would like to thank *Alex-Xianghua Zhou*, for all his help, support and guidance in almost everything during my initial stages. Without your guidance, I would have not been in this place. Thanks to *Chandu Ala*, my exceptional master's student, for his help on my projects. *Rajesh Kumar Nallapalli*, for his initial support and brotherly love when I moved to Gothenburg. Thank you all for sharing your

friendship, knowledge and happy occasions we enjoyed together. I would like to thank *Reza Salami, Sravani Devarakonda, Sevtap Gökalp, Çağlar Çil* and *Ali Alvandian*, who have supported me and created a friendly, enthusiastic atmosphere in the lab.

I would like to thank my co-supervisor, *Martin O Bergö*, for the collaborative work and fruitful discussions. Thanks for letting me use the instruments and reagents at the Sahlgrenska Cancer Center whenever needed. Special thanks to *Murali Krishna Akula*, for helping me with many experiments and personally as well. Thanks for the friendly attitude and making me feel at home in Gothenburg. I would like to thank *Christin Karlsson* for her help with the Mirax scanner and irradiation system for bone marrow transplantation.

I would like to thank *Jan Borén*, for extremely stimulating collaboration, for opening your group to me, for all the resources you allowed me to use at the Wallenberg Laboratory. I would like to thank *Liliana Håversen*, for all the exciting discussions and advices on lipid biology. I would like to thank *Kristina Skålen*, for animal experiments, *Elin Stenfeldt* for lipid fractionation analysis, *Max Levin* and *Matias Ekstrand*, for the immunofluorescence stainings in the atherosclerosis project, *Samad Parhizkar*

and *Shahin de Lara*, for the histological analysis of mouse aortas at the Department of Clinical Pathology, *Erik Larsson* and *Joakim Karlsson*, for the bioinformatics analysis, *Elmir Ömerovic* and *Björn Redfors*, for performing MI in mice, *Julia Grönros*, for the UCG examinations, *Josefin Kjelldahl* and *Göran Bergström*, for providing human endarterectomy samples and *Abdullhussain Haamid*, for all the help at the Laboratory of Experimental Biomedicine, and *Jennifer Uhler*, for linguistic help.

I would like to thank my friends, especially *Mikael Ahlgren*, *Marodana Glogov*, *Mattias Faltsetas* and *Zulfi Syed*, for all the fun we had on fishing trips. My childhood friends *Ankal Reddy* and *Sundeep Talluri* and friends *Vijay Kumar* and *Pradeep kopparapu*, *Chilaka venkatesh* and *Juttu Srinivas* who always motivated me.

These studies were mainly supported by the generous grants from the *Swedish Cancer Foundation* and *ALF grants from the Västra Götaland Region*.

Finally, I would like to thank my family for their support and the inspiration they gave me to realize this huge goal. My dad, *Sekhar*, always by my side, even though you were hard on me on multiple occasions, in the end you always wanted me enjoy every moment in my life. My mother, *Subbalakshmi*, what can I say about you, it's hard just to say thanks for everything you have given me. I will always be your little boy. My cousins here, *Suman* and *Janani Akka*, thanks for making me feel at home here. My cousin, *Chaitu*, and my mama, *Ramana Reddy*, for giving me the precious gift of life. Last but not least, I owe my deepest thanks to my wife, *Srujana*, for all your love, patience and support in my life. My son, *Shriyan*, together with you, I have experienced the most wonderful moments in my life. I "love you".

Sashidhar Bandaru

Göteborg, November 2018

References

1. Wang, K., J.F. Ash, and S.J. Singer, *Filamin, a new high-molecular-weight protein found in smooth muscle and non-muscle cells*. Proc Natl Acad Sci U S A, 1975. 72: 4483–4496.
2. Guo, Y., et al., *Physical and genetic interaction of filamin with presenilin in Drosophila*. J Cell Sci, 2000. 113 Pt 19: 3499–3508.
3. van der Flier, A. and A. Sonnenberg, *Structural and functional aspects of filamins*. Biochim Biophys Acta, 2001. 1538: 99–117.
4. Lu, J., et al., *Filamin B mutations cause chondrocyte defects in skeletal development*. Hum Mol Genet, 2007. 16: 1661–1675.
5. Zhou, X., J. Borén, and L.M. Akyürek, *Filamins in cardiovascular development*. Trends Cardiovasc Med, 2007. 17: 222–229.
6. Stossel, T.P., et al., *Filamins as integrators of cell mechanics and signalling*. Nature Reviews Mol Cell Biol, 2001. 2: 138–145.
7. Zhou, A.X., J.H. Hartwig, and L.M. Akyürek, *Filamins in cell signaling, transcription and organ development*. Trends Cell Biol, 2010. 20: 113–123.
8. Seo, M.D., et al., *Crystal structure of the dimerization domain of human filamin A*. Proteins, 2009. 75: 258–263.
9. Nakamura, F., et al., *Structural basis of filamin A functions*. J Cell Biol, 2007. 179: 1011–1025.
10. Lebart, M.C., et al., *Characterization of the actin binding site on smooth muscle filamin*. J Biol Chem, 1994. 269: 4279–4284.
11. Nakamura, F., T.P. Stossel, and J.H. Hartwig, *The filamins: organizers of cell structure and function*. Cell Adh Migr, 2011. 5(2): 160–169.
12. Lad, Y., et al., *Structure of three tandem filamin domains reveals auto-inhibition of ligand binding*. EMBO J, 2007. 26: 3993–4004.
13. Heikkinen, O.K., et al., *Atomic structures of two novel immunoglobulin-like domain pairs in the actin cross-linking protein filamin*. J Biol Chem, 2009. 284: 25450–25458.
14. Gardel, M.L., et al., *Prestressed F-actin networks cross-linked by hinged filamins replicate mechanical properties of cells*. Proc Natl Acad Sci U S A, 2006. 103: 1762–1767.
15. Fox, J.E., et al., *Identification of two proteins (actin-binding protein and P235) that are hydrolyzed by endogenous Ca²⁺-dependent protease during platelet aggregation*. J Biol Chem, 1985. 260: 1060–1066.
16. Savoy, R.M. and P.M. Ghosh, *The dual role of filamin A in cancer: can't live with (too much of) it, can't live without it*. Endocr Relat Cancer, 2013. 20: R341–356.
17. Muller, M., et al., *Localization of tissue factor in actin-filament-rich membrane areas of epithelial cells*. Exp Cell Res, 1999. 248: 136–147.
18. Feng, Y.Y., et al., *Filamin A (FLNA) is required for cell-cell contact in vascular development and cardiac morphogenesis*. Proc Natl Acad Sci U S A, 2006. 103: 19836–19841.

19. Cranmer, S.L., et al., *High shear-dependent loss of membrane integrity and defective platelet adhesion following disruption of the GPIIb/IIIa-filamin interaction*. *Blood*, 2011. 117: 2718–27.
20. Lian, G.W., et al., *Filamin A Regulates neural progenitor proliferation and cortical size through Wee1-Dependent Cdk1 phosphorylation*. *J Neurosci*, 2012. 32: 7672–7684.
21. Nagano, T., et al., *Filamin A-interacting protein (FILIP) regulates cortical cell migration out of the ventricular zone*. *Nat Cell Biol*, 2002. 4: 495–501.
22. Nagano, T., S. Morikubo, and M. Sato, *Filamin a and FILIP (Filamin A-interacting protein) regulate cell polarity and motility in neocortical subventricular and intermediate zones during radial migration*. *J Neurosci*, 2004. 24: 9648–9657.
23. Lu, J., et al., *Overlapping expression of ARFGEF2 and filamin a in the neuroependymal lining of the lateral ventricles: Insights into the cause of periventricular heterotopia*. *J Comp Neurol*, 2006. 494: 476–484.
24. Gay, O., et al., *RefilinB (FAM101B) targets filamin A to organize perinuclear actin networks and regulates nuclear shape*. *Proc Natl Acad Sci U S A*, 2011. 108: 11464–11479.
25. Sarkisian, M.R., et al., *MEKK4 signaling regulates filamin expression and neuronal migration*. *Neuron*, 2006. 52: 789–801.
26. Zhong, Z., et al., *Cyclin D1/cyclin-dependent kinase 4 interacts with filamin A and affects the migration and invasion potential of breast cancer cells*. *Cancer Res*, 2010. 70: 2105–2114.
27. Loy, C.J., K.S. Sim, and E.L. Yong, *Filamin-A fragment localizes to the nucleus to regulate androgen receptor and coactivator functions*. *Proc Natl Acad Sci U S A*, 2003. 100: 4562–4567.
28. Ozanne, D.M., et al., *Androgen receptor nuclear translocation is facilitated by the f-actin cross-linking protein filamin*. *Mol Endo*, 2000. 14: 1618–1626.
29. Meng, X., et al., *Recovery from DNA damage-induced G₂ arrest requires actin-binding protein filamin-A/actin-binding protein 280*. *J Biol Chem*, 2004. 279: 6098–6105.
30. van Vliet, A.R. and P. Agostinis, *PERK interacts with FLNA to regulate ER-PM contact sites*. *Oncotarget*, 2017. 8: 106155–106156.
31. Nallapalli, R.K., et al., *Targeting filamin A reduces K-RAS-induced lung adenocarcinomas and endothelial response to tumor growth in mice*. *Mol Cancer*, 2012. 11: 50.
32. Maceyka, M., et al., *Filamin A links sphingosine kinase 1 and sphingosine-1-phosphate receptor 1 at lamellipodia to orchestrate cell migration*. *Mol Cell Biol*, 2008. 28: 5687–5697.
33. Campos, L.S., et al., *Filamin A expression negatively regulates sphingosine-1-phosphate-induced NF- κ B activation in melanoma cells by inhibition of Akt signaling*. *Mol Cell Biol*, 2016. 36: 320–329.
34. Leonardi, A., et al., *Physical and functional interaction of filamin (actin-binding protein-280) and tumor necrosis factor receptor-associated factor 2*. *J Biol Chem*, 2000. 275: 271–278.
35. Campbell, I.D., *Studies of focal adhesion assembly*. *Biochem Soc Trans*, 2008. 36: 263–266.
36. Bellanger, J.M., et al., *The Rac1-and RhoG-specific GEF domain of Trio targets filamin to remodel cytoskeletal actin*. *Nat Cell Biol*, 2000. 2: 888–892.

37. Urban, E., et al., *Electron tomography reveals unbranched networks of actin filaments in lamellipodia*. Nat Cell Biol, 2010. 12: 429–435.
38. Kim, H., et al., *Filamin A regulates cell spreading and survival via β_1 integrins*. Exp Cell Res, 2008. 314: 834–846.
39. Glogauer, M., et al., *The role of actin-binding protein 280 in integrin-dependent mechanoprotection*. J Biol Chem, 1998. 273: 1689–1698.
40. Kim, H. and C.A. McCulloch, *Filamin A mediates interactions between cytoskeletal proteins that control cell adhesion*. Febs Letters, 2011. 585: 18–22.
41. Fox, J.W., et al., *Mutations in filamin 1 prevent migration of cerebral cortical neurons in human periventricular heterotopia*. Neuron, 1998. 21: 1315–1325.
42. Hart, A.W., et al., *Cardiac malformations and midline skeletal defects in mice lacking filamin A*. Hum Mol Genet, 2006. 15: 2457–2467.
43. Lammermann, T., et al., *Rapid leukocyte migration by integrin-independent flowing and squeezing*. Nature, 2008. 453: 51–55.
44. Barry, N.P. and M.S. Bretscher, *Dictyostelium amoebae and neutrophils can swim*. Proc Natl Acad Sci U S A, 2010. 107: 11376–11380.
45. Loo, D.T., S.B. Kanner, and A. Aruffo, *Filamin binds to the cytoplasmic domain of the β_1 -integrin. Identification of amino acids responsible for this interaction*. J Biol Chem, 1998. 273: 23304–23312.
46. Sharma, C.P., R.M. Ezzell, and M.A. Arnaout, *Direct interaction of filamin (ABP-280) with the β_2 -integrin subunit CD18*. J Immunol, 1995. 154: 3461–3470.
47. Calderwood, D.A., et al., *Increased filamin binding to β -integrin cytoplasmic domains inhibits cell migration*. Nat Cell Biol, 2001. 3: 1060–1068.
48. Mammoto, A., S. Huang, and D.E. Ingber, *Filamin links cell shape and cytoskeletal structure to Rho regulation by controlling accumulation of p190RhoGAP in lipid rafts*. J Cell Sci, 2007. 120: 456–467.
49. Heuze, M.L., et al., *ASB2 targets filamins A and B to proteasomal degradation*. Blood, 2008. 112: 5130–5140.
50. O'Connell, M.P., et al., *Wnt5A activates the calpain-mediated cleavage of filamin A*. J Invest Dermatol, 2009. 129: 1782–1789.
51. D'Addario, M., et al., *Cytoprotection against mechanical forces delivered through β_1 integrins requires induction of filamin A*. J Biol Chem, 2001. 276: 31969–31977.
52. Meyer, S.C., D.A. Sanan, and J.E.B. Fox, *Role of actin-binding protein in insertion of adhesion receptors into the membrane*. J Biol Chem, 1998. 273: 3013–3020.
53. Xu, Y.J., et al., *Filamin A regulates focal adhesion disassembly and suppresses breast cancer cell migration and invasion*. J Expl Med, 2010. 207: 2421–2437.
54. Flevaris, P., et al., *A molecular switch that controls cell spreading and retraction*. J Cell Biol, 2007. 179(3): 553–565.
55. Franco, S.J., et al., *Calpain-mediated proteolysis of talin regulates adhesion dynamics*. Nat Cell Biol, 2004. 6: 977–983.

56. Kim, H., et al., *Regulation of cell adhesion to collagen via β_1 integrins is dependent on interactions of filamin A with vimentin and protein kinase C epsilon*. *Exp Cell Res*, 2010. 316: 1829–1844.
57. Ohta, Y., et al., *The small GTPase RalA targets filamin to induce filopodia*. *Proc Natl Acad Sci U S A*, 1999. 96: 2122–2128.
58. Vadlamudi, R.K., et al., *Filamin is essential in actin cytoskeletal assembly mediated by p21-activated kinase 1*. *Nat Cell Biol*, 2002. 4: 681–690.
59. Pi, M., et al., *Calcium-sensing receptor activation of rho involves filamin and rho-guanine nucleotide exchange factor*. *Endocrinology*, 2002. 143: 3830–3838.
60. Ohta, Y., J.H. Hartwig, and T.P. Stossel, *FilGAP, a Rho- and ROCK-regulated GAP for Rac binds filamin A to control actin remodelling*. *Nat Cell Biol*, 2006. 8: 803–814.
61. Sasaki, A., et al., *Filamin associates with Smads and regulates transforming growth factor- β signaling*. *J Biol Chem*, 2001. 276: 17871–17877.
62. Yoshida, N., et al., *Filamin A-bound PEBP2 β /CBF β is retained in the cytoplasm and prevented from functioning as a partner of the Runx1 transcription factor*. *Mol Cell Biol*, 2005. 25: 1003–1012.
63. Kim, E.J., J.S. Park, and S.J. Um, *Filamin A negatively regulates the transcriptional activity of p73 α in the cytoplasm*. *Biochem Biophys Res Commun*, 2007. 362 : 1101–1106.
64. Yuan, Y. and Z. Shen, *Interaction with BRCA2 suggests a role for filamin-1 (hsFLNa) in DNA damage response*. *J Biol Chem*, 2001. 276: 48318–48324.
65. Berry, F.B., et al., *FOXC1 transcriptional regulatory activity is impaired by PBX1 in a filamin A-mediated manner*. *Mol Cell Biol*, 2005. 25: 1415–1424.
66. Wang, Y., et al., *A 90 kDa fragment of filamin A promotes Casodex-induced growth inhibition in Casodex-resistant androgen receptor positive C4-2 prostate cancer cells*. *Oncogene*, 2007. 26: 6061–6070.
67. Ozanne, D.M., et al., *Androgen receptor nuclear translocation is facilitated by the f-actin cross-linking protein filamin*. *Mol Endocrinol*, 2000. 14: 1618–1626.
68. Bruick, R.K., *Oxygen sensing in the hypoxic response pathway: regulation of the hypoxia-inducible transcription factor*. *Genes Dev*, 2003. 17: 2614–2623.
69. Bracken, C.P., M.L. Whitelaw, and D.J. Peet, *The hypoxia-inducible factors: key transcriptional regulators of hypoxic responses*. *Cell Mol Life Sci*, 2003. 60: 1376–1393.
70. Pugh, C.W. and P.J. Ratcliffe, *Regulation of angiogenesis by hypoxia: role of the HIF system*. *Nat Med*, 2003. 9: 677–684.
71. Ferrara, N., H.P. Gerber, and J. LeCouter, *The biology of VEGF and its receptors*. *Nat Med*, 2003. 9: p. 669–676.
72. Zheng, X., et al., *Hypoxia-induced and calpain-dependent cleavage of filamin A regulates the hypoxic response*. *Proc Natl Acad Sci U S A*, 2014. 111: 2560–2565.
73. Zhou, A.X., et al., *Filamin a mediates HGF/c-MET signaling in tumor cell migration*. *Int J Cancer*, 2011. 128: 839–846.
74. Birchmeier, C., et al., *Met, metastasis, motility and more*. *Nat Rev Mol Cell Biol*, 2003. 4: 915–925.

75. Zhang, Y.W. and G.F. Vande Woude, *HGF/SF-met signaling in the control of branching morphogenesis and invasion*. J Cell Biochem, 2003. 88: 408–417.
76. Wegenka, U.M., et al., *Acute-Phase Response Factor, a Nuclear Factor Binding to Acute-Phase Response Elements, Is Rapidly Activated by Interleukin-6 at the Posttranslational Level*. Mol Cellular Biol, 1993. 13: 276–288.
77. Takeda, K., et al., *Targeted disruption of the mouse Stat3 gene leads to early embryonic lethality*. Proc Natl Acad Sci U S A, 1997. 94: 3801–3804.
78. Levy, D.E. and C.K. Lee, *What does Stat3 do?* J Clin Invest, 2002. 109: 1143–1148.
79. Guschin, D., et al., *A major role for the protein tyrosine kinase JAK1 in the JAK/STAT signal transduction pathway in response to interleukin-6*. EMBO J, 1995. 14: 1421–1429.
80. Benekli, M., et al., *Signal transducer and activator of transcription proteins in leukemias*. Blood, 2003. 101: 2940–2954.
81. Dutzmann, J., et al., *Emerging translational approaches to target STAT3 signalling and its impact on vascular disease*. Cardiovasc Res, 2015. 106: 365–374.
82. Harada, M., et al., *G-CSF prevents cardiac remodeling after myocardial infarction by activating the Jak-Stat pathway in cardiomyocytes*. Nat Med, 2005. 11: 305–311.
83. Hilfiker-Kleiner, D., et al., *Signal transducer and activator of transcription 3 is required for myocardial capillary growth, control of interstitial matrix deposition, and heart protection from ischemic injury*. Circ Res, 2004. 95: 187–195.
84. Zhou, X.X., et al., *Pravastatin prevents aortic atherosclerosis via modulation of signal transduction and activation of transcription 3 (STAT3) to attenuate interleukin-6 (IL-6) action in ApoE knockout mice*. Int J Mol Sci, 2008. 9: 2253–2264.
85. Ridker, P.M., et al., *Plasma concentration of interleukin-6 and the risk of future myocardial infarction among apparently healthy men*. Circulation, 2000. 101: 1767–1772.
86. Gan, A.M., et al., *Monocytes and smooth muscle cells cross-talk activates STAT3 and induces resistin and reactive oxygen species production*. J Cell Biochem, 2013. 114: 2273–2283.
87. Loppnow, H., et al., *Statins potently reduce the cytokine-mediated IL-6 release in SMC/MNC cocultures*. J Cell Mol Med, 2011. 15: 994–1004.
88. Sorimachi, H., S. Hata, and Y. Ono, *Impact of genetic insights into calpain biology*. J Biochem, 2011. 150: 23–37.
89. Sorimachi, H., S. Hata, and Y. Ono, *Expanding Members and Roles of the Calpain Superfamily and Their Genetically Modified Animals*. Exp Animals, 2010. 59: 549–566.
90. Ohno, S., et al., *Evolutionary Origin of a Calcium-Dependent Protease by Fusion of Genes for a Thiol Protease and a Calcium-Binding Protein*. Nature, 1984. 312: 566–570.
91. Davies, P.J., et al., *Filamin-actin interaction. Dissociation of binding from gelation by Ca²⁺-activated proteolysis*. J Biol Chem, 1978. 253: 4036–4042.
92. Hemmings, L., et al., *Talin contains three actin-binding sites each of which is adjacent to a vinculin-binding site*. J Cell Sci, 1996. 109: 2715–2726.

93. Arthur, J.S., et al., *Disruption of the murine calpain small subunit gene, Capn4: calpain is essential for embryonic development but not for cell growth and division*. Mol Cell Biol, 2000. 20: 4474–4481.
94. Kishimoto, A., et al., *Limited proteolysis of protein kinase C subspecies by calcium-dependent neutral protease (calpain)*. J Biol Chem, 1989. 264: 4088–4092.
95. Kidd, V.J., J.M. Lathi, and T. Teitz, *Proteolytic regulation of apoptosis*. Sem Cell Dev Bio, 2000. 11: 191–201.
96. Pariat, M., et al., *The sensitivity of c-Jun and c-Fos proteins to calpains depends on conformational determinants of the monomers and not on formation of dimers*. Biochem J, 2000. 345: 129–138.
97. Watanabe, N., et al., *Specific Proteolysis of the C-Mos Proto-Oncogene Product by Calpain on Fertilization of Xenopus Eggs*. Nature, 1989. 342: 505–511.
98. Donkor, I.O., *An updated patent review of calpain inhibitors (2012 - 2014)*. Expert Opin Ther Pat, 2015. 25: 17–31.
99. Ozaki, T., et al., *Intravitreal injection or topical eye-drop application of a mu-calpain C2L domain peptide protects against photoreceptor cell death in Royal College of Surgeons' rats, a model of retinitis pigmentosa*. Biochim Biophys Acta, 2012. 1822: 1783–1795.
100. Sanderson, J., J.M. Marcantonio, and G. Duncan, *A human lens model of cortical cataract: Ca²⁺-induced protein loss, vimentin cleavage and opacification*. Invest Ophthalmol Vis Sci, 2000. 41: 2255–2261.
101. Lee, E., et al., *Neuroprotective effect of undecylenic acid extracted from Ricinus communis L. through inhibition of μ -calpain*. Eur J Pharm Sci, 2012. 46: 17–25.
102. Baghdiguian, S., et al., *Calpain 3 deficiency is associated with myonuclear apoptosis and profound perturbation of the I κ B α /NF- κ B pathway in limb-girdle muscular dystrophy type 2A*. Nat Med, 1999. 5: 503–511.
103. Ilian, M.A., R.S. Gilmour, and R. Bickerstaffe, *Quantification of ovine and bovine calpain I, calpain II, and calpastatin mRNA by ribonuclease protection assay*. J Anim Sci, 1999. 77: 853–864.
104. Inserte, J., V. Hernando, and D. Garcia-Dorado, *Contribution of calpains to myocardial ischaemia/reperfusion injury*. Cardiovasc Res, 2012. 96: 23–31.
105. Cunningham, C.C., et al., *Actin-binding protein requirement for cortical stability and efficient locomotion*. Science, 1992. 255: 325–337.
106. Retailleau, K., et al., *Smooth muscle filamin A is a major determinant of conduit artery structure and function at the adult stage*. Pflugers Arch, 2016. 468: 1151–1160.
107. Begonja, A.J., et al., *FlnA-null megakaryocytes prematurely release large and fragile platelets that circulate poorly*. Blood, 2011. 118: 2285–2295.
108. Leung, R., et al., *Filamin A regulates monocyte migration through Rho small GTPases during osteoclastogenesis*. J Bone Miner Res, 2010. 25: 1077–1091.
109. Disease, G.B.D., I. Injury, and C. Prevalence, *Global, regional, and national incidence, prevalence, and years lived with disability for 310 diseases and injuries, 1990-2015: A systematic analysis for the Global Burden of Disease Study 2015*. Lancet, 2016. 388: 1545–1602.

110. Van de Werf, F., et al., *Management of acute myocardial infarction in patients presenting with persistent ST-segment elevation: the Task Force on the Management of ST-Segment Elevation Acute Myocardial Infarction of the European Society of Cardiology*. Eur Heart J, 2008. 29: 2909–2945.
111. Buja, L.M., *Myocardial ischemia and reperfusion injury*. Cardiovasc Pathol, 2005. 14: 170–175.
112. Kutty, R.S., N. Jones, and N. Moorjani, *Mechanical complications of acute myocardial infarction*. Cardiol Clin, 2013. 31: 519–531.
113. O'Gara, P.T., et al., *2013 ACCF/AHA guideline for the management of ST-elevation myocardial infarction: A report of the American College of Cardiology Foundation/American Heart Association Task Force on Practice Guidelines*. Circulation, 2013. 127: e362–425.
114. Sumpio, B.E., J.T. Riley, and A. Dardik, *Cells in focus: endothelial cell*. Int J Biochem Cell Biol, 2002. 34: 1508–1512.
115. Sasayama, S. and M. Fujita, *Recent insights into coronary collateral circulation*. Circulation, 1992. 85: 1197–1204.
116. Hansson, G.K., *Inflammatory mechanisms in atherosclerosis*. J Thromb Haemost, 2009. 7 Suppl 1: 328–331.
117. Hansson, G.K., *Atherosclerosis--an immune disease: The Anitschkov Lecture 2007*. Atherosclerosis, 2009. 202: 2–10.
118. Wick, G. and Q. Xu., *Atherosclerosis--an autoimmune disease*. Exp Gerontol, 1999. 34: 559–566.
119. Ross, R. and J.A. Glomset, *Atherosclerosis and the arterial smooth muscle cell: Proliferation of smooth muscle is a key event in the genesis of the lesions of atherosclerosis*. Science, 1973. 180: 1332–1339.
120. Williams, K.J. and I. Tabas, *The response-to-retention hypothesis of atherogenesis reinforced*. Curr Opin Lipidol, 1998. 9: 471–474.
121. Williams, K.J. and I. Tabas, *The response-to-retention hypothesis of early atherogenesis*. Arterioscler Thromb Vasc Biol, 1995. 15: 551–561.
122. Ross, R., *Atherosclerosis--an inflammatory disease*. N Engl J Med, 1999. 340: 115–126.
123. Ovchinnikov, D.A., *Macrophages in the embryo and beyond: Much more than just giant phagocytes*. Genesis, 2008. 46: 447–462.
124. Oh, J., et al., *Endoplasmic reticulum stress controls M2 macrophage differentiation and foam cell formation*. J Biol Chem, 2012. 287: 11629–11641.
125. Saric, M. and I. Kronzon, *Aortic atherosclerosis and embolic events*. Curr Cardiol Rep, 2012. 14: 342–349.
126. Robertson, S.P., et al., *Frontometaphyseal dysplasia: Mutations in FLNA and phenotypic diversity*. Am J Med Gen A, 2006. 140: 2840–2840.
127. Robertson, S.P., et al., *Localized mutations in the gene encoding the cytoskeletal protein filamin A cause diverse malformations in humans*. Nat Gen, 2003. 33: 487–491.
128. Feng, Y. and C.A. Walsh, *The many faces of filamin: a versatile molecular scaffold for cell motility and signalling*. Nat Cell Biol, 2004. 6: 1034–1138.
129. Kyndt, F., et al., *Mutations in the gene encoding filamin A as a cause for familial cardiac valvular dystrophy*. Circulation, 2007. 115: 40–49.

130. Parrini, E., et al., *Periventricular heterotopia: phenotypic heterogeneity and correlation with Filamin A mutations*. Brain, 2006. 129: 1892–1906.
131. Sheen, V.L., et al., *Filamin A mutations cause periventricular heterotopia with Ehlers-Danlos syndrome*. Neurology, 2005. 64: 254–262.
132. Khan, O.M., et al., *Targeting GGTase-1 activates RHOA, increases macrophage reverse cholesterol transport, and reduces atherosclerosis in mice*. Circulation, 2013. 127:782–790.
133. Tian, F., et al., *Endothelial cells are activated during hypoxia via endoglin/ALK-1/SMAD1/5 signaling in vivo and in vitro*. Biochem Biophys Res Commun, 2010. 392: 283–238.
134. Tian, F., et al., *Protein disulfide isomerase increases in myocardial endothelial cells in mice exposed to chronic hypoxia: a stimulatory role in angiogenesis*. Am J Physiol Heart Circ Physiol, 2009. 297: H1078–1086.
135. Fagerberg, B., et al., *Differences in lesion severity and cellular composition between in vivo assessed upstream and downstream sides of human symptomatic carotid atherosclerotic plaques*. J Vasc Res, 2010. 47: 221–230.
136. Ekstrand, M., et al., *Depletion of ATP and glucose in advanced human atherosclerotic plaques*. PLoS One, 2017. 12: e0178877.
137. Alva, J.A., et al., *VE-Cadherin-Cre-recombinase transgenic mouse: a tool for lineage analysis and gene deletion in endothelial cells*. Dev Dyn, 2006. 235: 759–767.
138. Clausen, B.E., et al., *Conditional gene targeting in macrophages and granulocytes using LysMcre mice*. Transgenic Res, 1999. 8: 265–277.
139. Lundqvist, A., et al., *Oregonin reduces lipid accumulation and proinflammatory responses in primary human macrophages*. Biochem Biophys Res Commun, 2015. 458: p. 693–699.
140. Bandaru, S., et al., *Deficiency of filamin A in endothelial cells impairs left ventricular remodelling after myocardial infarction*. Cardiovasc Res, 2015. 105: 151–159.
141. Sayin, V.I., et al., *Loss of one copy of Zfp148 reduces lesional macrophage proliferation and atherosclerosis in mice by activating p53*. Circ Res, 2014. 115: 781–789.
142. Björklund, M.M., et al., *Induction of atherosclerosis in mice and hamsters without germline genetic engineering*. Circ Res, 2014. 114: 1684–1692.
143. Ho, V.C., et al., *Elevated vascular endothelial growth factor receptor-2 abundance contributes to increased angiogenesis in vascular endothelial growth factor receptor-1-deficient mice*. Circulation, 2012. 126: 741–752.
144. Wang, Y., et al., *Ephrin-B2 controls VEGF-induced angiogenesis and lymphangiogenesis*. Nature, 2010. 465: 483–486.
145. Li, A.C. and C.K., Glass, *The macrophage foam cell as a target for therapeutic intervention*. Nat Med, 2002. 8: 1235–1242.
146. Akita, K., et al., *An interleukin-6 receptor antibody suppresses atherosclerosis in atherogenic mice*. Front Cardiovasc Med, 2017. 4: 84.
147. Cheng, F., et al., *A critical role for STAT3 signaling in immune tolerance*. Immunity, 2003. 19: 425–436.